SSD 79-0082

STAR-RAKER
AN AIRBREATHER/ROCKET-POWERED, HORIZONTAL TAKEOFF TRIDELTA FLYING WING, SINGLE-STAGE-TO-ORBIT TRANSPORTATION SYSTEM

By
David A. Reed, Jr.
Hideo Ikawa
Jonas A. Sadunas

Prepared for presentation at the AIAA Conference on
Advanced Technology for Future Space Systems
Hampton, Virginia

May 8-11, 1979

STAR-RAKER
AN AIRBREATHER/ROCKET-POWERED, HORIZONTAL TAKEOFF TRIDELTA FLYING WING, SINGLE-STAGE-TO-ORBIT TRANSPORTATION SYSTEM

David A. Reed, Jr.*, Hideo Ikawa*, Jonas A. Sadunas*

Abstract

Star-Raker is a versatile space transportation system (STS) that eliminates the need for expensive launch facilities, vehicle assembly buildings, and expendable boosters. It is a system that can operate from any large airport equipped with cryogenic facilities, can carry a 100-ton payload into any 556-km (300 nmi) orbit, uses multicycle airbreather propulsion, and is lightweight. These qualities contribute to operational flexibility, and can play key roles in fulfilling future earth/space transportation requirements.

Introduction

Studies conducted by NASA and industry[1,2] have clearly established the need for a new earth launch vehicle (ELV) if the satellite power systems (SPS's) are to be economically viable. Typically, the ELV's conceived to meet this need are vertically launched and fully recoverable. To be cost-effective, they must transport very large payloads (100,000 kg or more) to orbit. These concepts, although based on acceptable technology, introduce uncertainties related to major program planning and operational usage.

Development of large ELV's can be justified only in the context of full SPS production go-ahead. This is dictated by the substantial funding required for development of vehicles and launch facilities whose projected applicability is limited solely to the demands of an SPS program. A potential funding dilemma is posed if a near full-scale prototype SPS at geosynchronous orbit is required for proof of concept, inasmuch as a new ELV could save billions of dollars in launch operations costs if it were available. What is needed, therefore, is an ELV concept that offers the potential of low dollars per pound to orbit and is also applicable to future NASA and Air Force programs with considerably lesser demands than SPS. Thus, the economic risk of early development would be essentially negated.

Operationally, the concept of very large, vertically launched, all-rocket, boosters poses formidable environmental and logistical concerns. Atmospheric and launch acoustics pollution will be high for the multiple-launches-per-day requirements. Water recovery of expended ballistic stages and subsequent refurbishment, stacking, payload integration, and countdowns with short turnaround schedules at low cost represent a solution full of credibility issues for launch systems recovery. There is a need, therefore, for a new ELV concept which can counter many of these objections.

While conducting the Satellite Power System (SPS) Concept Definition Study (NAS8-32161), Rockwell introduced a horizontal takeoff, tridelta flying wing configuration spacecraft, identified "Star-Raker."** This spacecraft is powered with turbofan, air turbo exchanger, ramjet multicycle airbreather engines, and rocket engines. The configuration, weights, and performance estimates for this vehicle were based on 1968 preliminary conceptual efforts prior to the Space Shuttle procurement. Justification for introducing the concept into the recently completed SPS study was founded on ROM cost correlations and the obvious operational advantages of such a system if it is proved feasible.

Previous investigations at Rockwell,† such as 1958 Navaho follow-on applications, Dyna-Soar, and initial recoverable orbital carrier (ROC) studies, included turbojet/ramjet propulsion limited to 10,660 m (35,000 ft) altitude and Mach 3 velocity. The studies included winged vehicles; however, the wings were not permitted to contain cryogenic propellants. The resultant maneuver from Mach 3 low-gamma (flight path angle), high-specific impulse (I_{sp}) flight inherent in aero propulsion to the high-gamma, low I_{sp} flight inherent in rocket propulsion negated most of the high I_{sp} potential of aero propulsion.

Later, recoverable orbital carrier studies increased airbreather propulsion up to Mach 6, using SWAT-201 high-bypass supersonic turbofan/ramjets. However, as in previous studies, wet wing designs were not permitted. The results of such designs indicated airbreather propulsion was of significant advantage for two-stage launch systems and marginal for single-stage launch systems.

"A-BALL" studies in 1968 and 1969 permitted wet wing design of "conventional" wing/body systems. Center-of-aerodynamic-pressure (c.p.) excursion across all Mach ranges proved to be excessive. However, the potential of single-stage-to-orbit launch systems was reasonably established. A review of supersonic transport (SST) studies conducted by Rockwell, Boeing, and Lockheed produced approximately 15 candidate planform systems with low c.p. excursions. The tridelta used in the Star-Raker design had the best c.p. versus Mach number behavior, and was chosen for further study in 1970.

The results of the 1970 Rockwell studies and the SPS transportation requirements from a NASA contract in 1976 were used as inputs for the 1977 IRDA activities. Data generated in 1977 provided a technology base for on-going 1978 study effort. This paper presents an overview of a reference vehicle, including system descriptions and data summaries, for IR&D studies ending in 1978.

Operational Features

The Star-Raker concept adapts existing and advanced commercial and/or military air transport system concepts, operations methods, maintenance procedures, and cargo handling equipment to include a space-related environment. The principal operational objective is to provide economical, reliable transportation of large quantities of material between earth and low earth orbit (LEO) at high flight frequencies with routine logistics operations and minimal environmental impact. An associated operational objective is to reduce the number of operations required to transport material and equipment from their place of manufacture on earth to low earth orbit. Goals for the Star-Raker concept, which are in addition to the quantitative requirements for logistic support of the SPS, include both NASA and Air Force objectives and requirements, such as the following.

*Members of Technical Staff, Advanced Systems Engineering Members AIAA

**Advanced system research activities of D.A. Reed, Jr., from 1958 to 1978. Star-Raker concept invented by Mr. Reed in 1968.

†At that time Rockwell was called North American Aviation, Inc.

- Total vehicle reusability–with many reuses
- Rapid turnaround
- Ferry capability with cargo between airfields
- Minimized launch costs
- High reliability of delivery
- Ability to reach any LEO plane from alternate launch sites (KSC, VAFB, and others) and return to the same site, including single-pass orbits
- Cargo security

Operational features derived in the study include:

- Single orbit up/down, from/to the same launch site (at any launch azimuth subject to payload/launch azimuth match)
- Capability of attaining a 556 km (300 nmi) equatorial orbit when launched from KSC
- Takeoff and landing on 2440- to 4270-m (8000- to 14,000-ft) runways (launch velocity ≈ 225 knots; landing velocity ≤ 115 knots)
- Simultaneous multiple launch
- Total system recovery, including jettison and recovery of takeoff gear at the launch site
- Payload cost potential of $22 to $33 per kilogram ($10 to $15 per pound) in 556-km (300-mni) orbits
- Negligible launch site refurbishment
- Powered landing from orbital reentry at any commercial or military airport capable of 747 or C-5A operations
- Aerodynamic flight capability from the payload manufacturing site to the launch site, addition of launch gear and fueling, and launch into earth orbit
- Amenability to alternative launch and landing sites
- Incorporation of Air Force (C-5A Galaxy) and commercial (747 cargo) payload handling, including railroad, truck, and cargo-ship containerization concepts, modified to meet space environment requirements
- Swing-nose loading and unloading, permitting the use of a normal aircraft loading-door facility
- Propulsion system service using existing support equipment on runway aprons or near service hangars
- In-flight refueling options (options not included in reference vehicle data)

Fig. 1 shows a Star-Raker vehicle in an airport alongside a Boeing 747 passenger plane. Multiple launch capability (shown in Fig. 2) combined with orbital operations (Fig. 3), and powered landing at commercial airports (shown in Fig. 4) illustrate the versatile attributes of flight for earth/space missions. Cargo loading, exemplified in Fig. 5, illustrates not only space operations but suborbital point-to-point earth operations that accrue as fall-out from the basic mission capabilities.

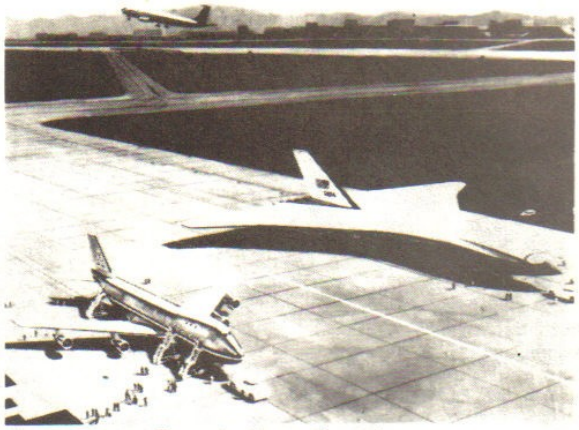

Figure 1. Airport Operations

Figure 2. Multiple Launch

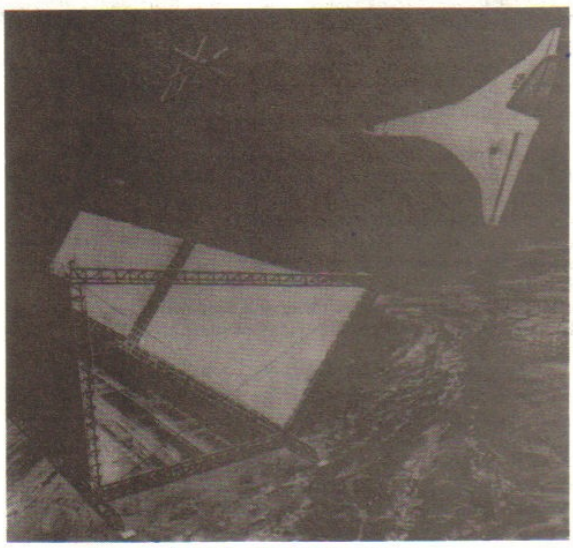

Figure 3. Orbital Operations

Design Features

The Star-Raker utilizes a tridelta flying wing, consisting of a multi-cell pressure vessel of tapered, intersecting cones. The tridelta planform and a Whitcomb airfoil section offer an efficient aerodynamic shape from a performance standpoint and high propellant volumetric efficiency. The outer panels of the wing and vent system lines in the wing's leading edge provide the gaseous

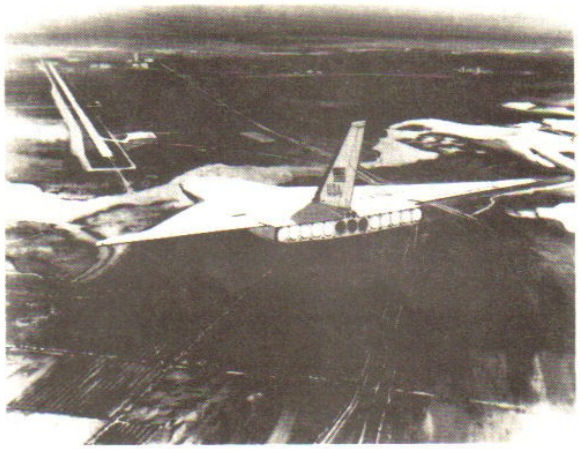

Figure 4. Powered Landing at Commercial Airport

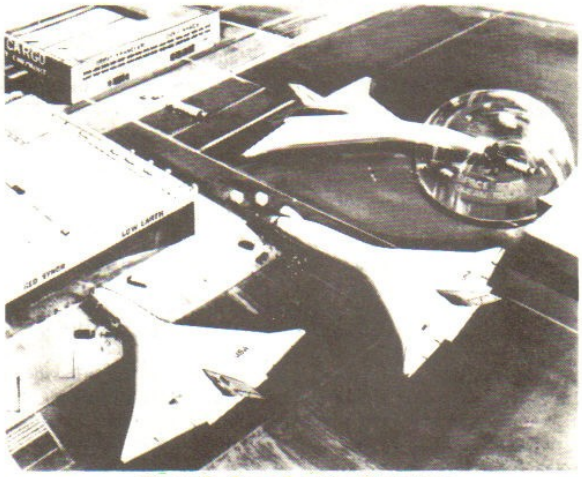

Figure 5. Cargo Loading Operations

ullage space for LH_2 fuel. LH_2 and LO_2 tanks are located in each wing about the vehicle center of gravity, and extend from the root rib to the wing-tip LH_2 ullage tank (Fig. 6). Approximately 20% of the volume of the vertical stabilizer is utilized as part of the gaseous ullage volume of the integral wing-mounted LO_2 tanks. In the aft end of the vehicle, three uprated high-P_c rocket engines (thrust = 14.24×10^6 newtons) are attached with a double-cone thrust structure to a two-cell LH_2 tank.

Most of the cargo bay side walls are provided by the root-rib bulkhead of the wing tanks. The cargo bay floor design is similar to that of the C5-A military transport aircraft. This permits the use of MATS and Airlog cargo loading and retention systems. The top of the cargo bay is a mold-line extension of the wing upper contours, wherein the frame inner caps are arched to resist pressure at minimum weight. The forward end of the cargo bay has a circular seal/docking provision to the forebody. Cargo is deployed in orbit by swinging the forebody 90 or more degrees about a vertical axis at the side of the seal and transferring cargo from the bay into space or to in-space receivers on telescoping rails. Over 85% of the mold-line volume is utilized for some useful purpose.

The forebody is an RM-10 ogive of revolution with an aft dome closure. The ogive is divided horizontally into two levels. The upper level provides seating for crew and passengers, as well as the flight deck. The lower compartment contains electronic, life

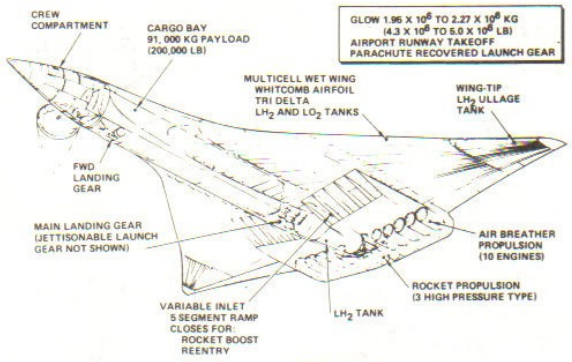

Figure 6. Star-Raker Design Features

support, power (fuel cell), and other subsystems, including spare life support and emergency recovery equipment.

Ten high-bypass, supersonic-turbofan/air-turbo-exchanger/ramjet airbreather engines with a combined static thrust of 6,227,510 N (1,400,000 lb) are mounted under the wing. The inlets are variable-area retractable ramps that also close and fair the bottom into a smooth surface during rocket powered flight and for either Sanger skip glider or high angle-of-attack initial reentry with atmospheric maneuverable descent.

Fig. 7 shows an inboard profile of the vehicle, illustrating the details of body construction, crew compartment, cargo bay length, LH_2 tank configuration, and location of the rocket engines at rear of fuselage. The hinging and rotation of the nose section for loading and unloading the payloads are illustrated, with indication of view angle from the rear of the nose section during these operations. The multiple landing gear concept shows the position of the nose gear bogie, the jettisonable takeoff gear, and the main landing gear for powered landing.

Fig. 8 presents front and rear views of the vehicle, showing the blended wing, engine inlet ducts, landing gear arrangement, and vertical stabilizer. Also shown are typical sections through the vehicle at the following places:

- The hinge line section (B-B) aft of the crew compartment and forward of the nose gear. Cross-sectional dimensions of the cargo bay are indicated.
- The 40% chord line fuselage section (C-C) illustrating the wing and fuselage construction and the profile of the wing/fuselage fairing.
- The main landing gear station (D-D) illustrating the gear retraction geometry, and the relationship of the gear to the engine air inlet ducts, and the wing construction and profile to the fuselage shape.

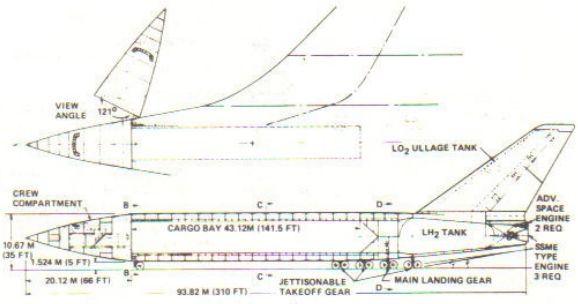

Figure 7. Star-Raker Inboard Profile

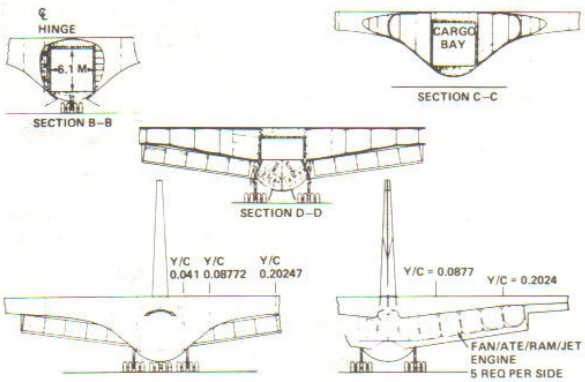

Figure 8. Vehicle Section

The multi-cell wing tank shown in Fig. 9 and enlarged construction details of Fig. 10 show how the aerodynamic lift, propellant pressure vessel, and thermal protection system requirements are integrated into a single, lightweight design concept.

Fig. 10 presents details of the basic multicell structure of the Star-Raker wing. The upper portion illustrates the application of Shuttle-type RSI tile thermal protection system (TPS), and the lower portion shows a potential utilization of a "metallic" TPS.

The wing is an integrated structural system consisting of an inner multi-cell pressure vessel, a foam-filled structural core, an inner facing sheet, a perforated structural honeycomb core, and an outer facing sheet. The inner multi-cell pressure vessel arched shell and webs are configured to resist pressure. The pressure vessel and the two facing sheets, which are structurally interconnected with phenolic-impregnated, glass-fiber, honeycomb core, resist wing spanwise and chordwise bending moments. Cell webs react wing-lift shear forces. Torsion is reacted by the pressure vessel and the two facing sheets as a multi-box wing structure.

The outer honeycomb core is perforated and partitioned to provide a controlled passage for purge and gas leak detection as well as a structural interconnect of the inner and outer facing sheets. The construction of the wing structure utilizes the "Inflation Assembly Technique" developed by Rockwell for the Saturn II booster common bulkhead.

Multi-Cycle Airbreather Engine System

Takeoff and climb to 30,400-km (100,000-ft) altitude and 1768 m/s (5800 ft/s) velocity are accomplished by airbreather propulsion. Parallel burn of airbreather and rocket propulsion occurs between 1768 to 2195 m/s (5800 to 7200 ft/s). Rocket power propels Star-Raker from 2195 m/s (7200 ft/s) into orbit.

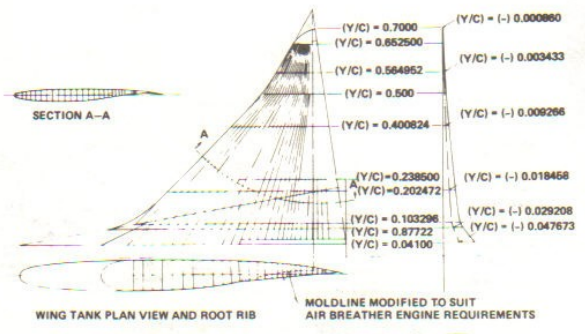

Figure 9. Multi-Cell Wing Tank Diagram

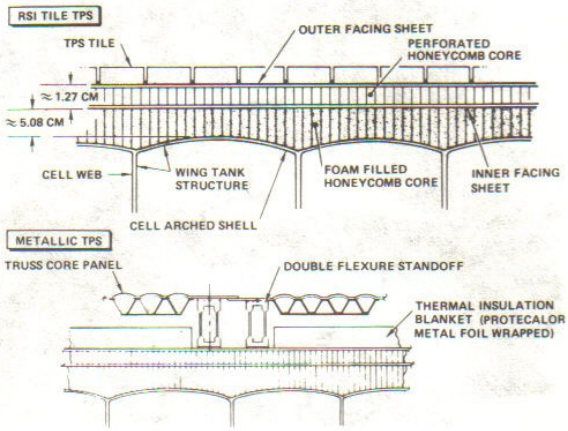

Figure 10. Wing Construction Detail With Candidate TPS Configuration

The multi-cycle airbreathing engine system concept (Fig. 11) is derived from the General Electric CJ805 aircraft engine, the Pratt and Whitney SWAT 201 supersonic wraparound turbofan/ramjet engine, the Aerojet Air Turborocket, the Marquardt variable plug-nozzle, ramjet engine technology, and the Rocketdyne tubular-cooled, high P_c rocket engine technology.

The multi-mode power cycles include an aft-fan, turbofan cycle; an LH_2, regenerative Rankine, air-turbo-exchanger cycle; and a ramjet cycle that can also be used as a full flow (turbojet core and fan bypass flow), thrust-augmented turbofan cycle. These four thermal cycles may receive fuel in any combination, permitting high engine performance over a flight profile from sea-level takeoff to Mach 6 at 30,400-km (100,000-ft) altitude.

The engine air inlet and duct system (Fig. 11) is based on a five-ramp variable inlet system with actuators to provide ramp movement from fully closed (upper right figure) for rocket-powered and reentry flight, to fully open (lower right figure) for takeoff operation.

The engine components include a rotary vane assembly to close off the compressor-turbine assembly at higher Mach numbers. LH_2 fuel permits the use of a Rankine-cycle air turbo-exchanger cycle to provide power for the bypass fan. This allows elimination of approximately one-half of the turbofan compressor stages normally needed for fan drive. Heating of the LH_2 in outer walls and nozzle plug of tubular construction, in addition to providing fan-drive power, permits stoichiometric combustion in the augmentor/ramjet by cooling of exposed surfaces. The 3055°K combustion temperature provides high cycle efficiency.

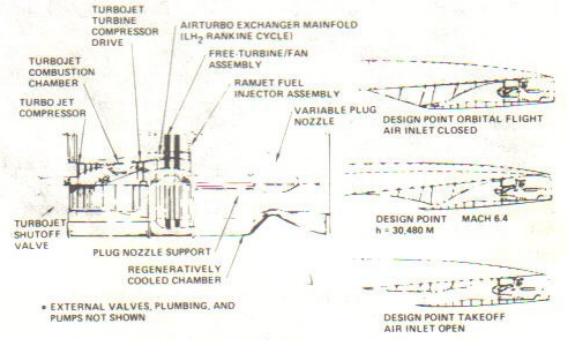

Figure 11. Multi-Cycle Airbreathing Engine and Inlet, Turbofan/Air Turboexchanger/Ramjet

The study scope did not permit a detailed evaluation of engine components to provide further, more accurate calculation of the performance capability of this engine concept. Engine manufacturers are best equipped to further refine the design and provide real data on concept feasibility and system weight.

The inlet area was determined by the engine airflow required at the Mach 6 design point. The configuration required 6,227,510 N (1.4×10^6 lb) of thrust at the Mach 6 condition and at least 5,337,870 N (1.2×10^6 lb) of thrust for takeoff. This resulted in an inlet area of approximately 111 m^2 (1200 ft^2), or 11.1 m^2 (120 ft^2) per engine for a 10-engine configuration. To provide pressure recovery with minimum spillage drag over the wide range of Mach numbers, a variable multi-ramp inlet is required. Inlet pressure recovery efficiency versus velocity is plotted on Fig. 12. Higher recoveries are possible for the Star-Raker than for military aircraft, which must operate during more violent maneuvers. However, the pressure recovery must still provide a margin which prevents inlet instability and possible engine flameout from expulsion of the normal shock during transients.

Estimated engine thrust (total of 10 engines) versus velocity is plotted on Fig. 13. Initially, a constant thrust of 6,227,510 N (1,400,000 lb) was assumed for the Rockwell modified Rutowski energy method trajectory analysis (dashed curve of Fig. 13). A tentative airbreather engine performance map was estimated from engine data sources previously described. The engine thrust versus Mach number estimate is shown by the upper solid curve of Fig. 13.

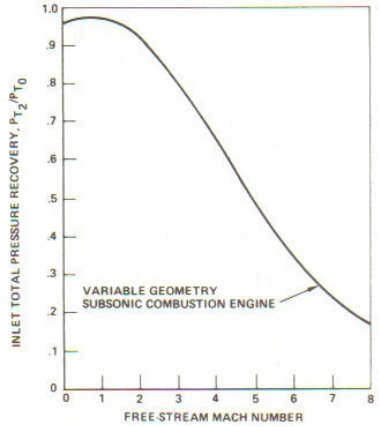

Figure 12. Air Induction System Performance

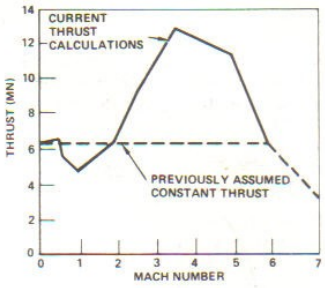

Figure 13. Airbreather Thrust Versus Mach Number

Typical I_{sp} characteristics of the AB/rocket engine system are:

- Subsonic range: Linear reduction of I_{sp} from 9700 to 4000 sec at 366 m/s (1200 ft/s)
- Supersonic range: Reduction of I_{sp} from 4000 sec at 366 m/s (1200 ft/s) to 3500 sec at ≈1707 m/s (5600 ft/s) (AB)
- Rocket: I_{sp} = 455 sec

Aerodynamic Characteristics

The wing shape is a supercritical Whitcomb airfoil with a relatively blunt leading edge, flat upper surfaces, and cambered trailing edges. The trailing-edge camber and the tridelta shape minimize translation of the center of pressure throughout the flight Mach number regime. The blunt leading edge offers good subsonic characteristics, but produces relatively high supersonic wave drag; therefore, further shape refinements are recommended. The wing has a spanwise thickness distribution of 10% at the root, 6% near midspan, and 5% at the tip, providing a large interior volume for storage of LH_2 and LO_2 propellants.

Subsonic and supersonic aerodynamic coefficients (C_L, C_D, c.p.) were calculated using the Flexible Unified Distributed Panel program. Aerodynamic coefficients computed at M_∞ = 5.0 were frozen and used for hypersonic application. Viscous drag due to the skin friction was added in a separate analysis. The resulting aerodynamic coefficients are plotted versus flight Mach number on Fig. 14.

Maximum lift/drag and corresponding lift coefficients and angle of attack versus Mach number are given on Fig. 15.

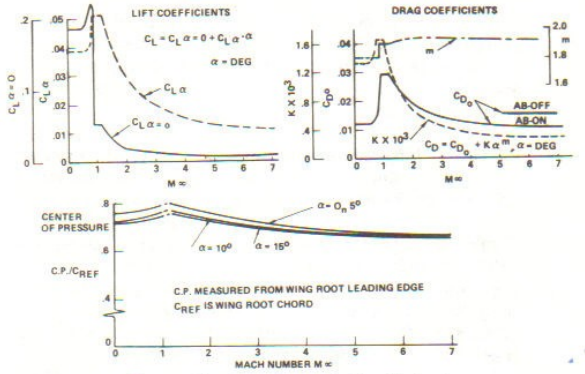

Figure 14. Aerodynamic Coefficients

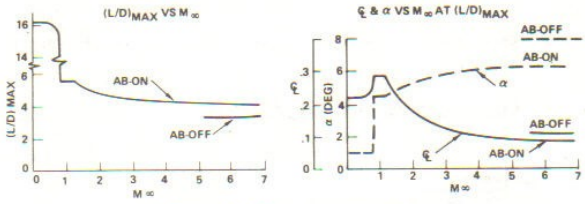

Figure 15. Maximum Lift/Drag

Flight Mechanics

Most of the ascent performance analyses for the Star-Raker vehicle concept were accomplished by employing the lifting ascent program which is based on a modified Rutowski energy method. A second computer program, the Two-Dimensional Trajectory Program (TDTP), was then used to compute the ascent trajectory timeline.

An end-to-end simulation of the Star-Raker (i.e., airbreather horizontal takeoff, climb, cruise, turn, airbreather ascent, rocket ascent, coast and final orbit insertion) with flight optimization including aerodynamic effects was verified by the Langley

Program to Optimize Simulated Trajectory (POST), developed by Martin-Marietta.

The Star-Raker uses aircraft-type flight from airport takeoff to approximately Mach 6, with a parallel burn transition of air-breather and rocket engines from Mach 6 to 7.2, and rocket-only burn from Mach 7.2 to orbit. Fig. 16 illustrates a nominal trajectory from KSC to 556-km (300-nmi) earth equatorial orbit. Prime elements of the trajectory include:

- Runway takeoff under high-pass turbofan/airturbo exchanger (ATE)/ramjet power, with the ramjets acting as supercharged afterburners
- Jettison and parachute recovery of landing gear used only for launch
- Climb to optimum cruise altitude with turbofan and ATE power
- Cruise at optimum altitude, Mach number, and direction vector to earth's equatorial plane, using turbofan power
- Execute a large radius turn into the equatorial plane with turbofan power
- Climb subsonically at optimum climb angle and velocity to an optimum altitude by using high bypass turbofan/ATE/ramjet (super-charged afterburner) power
- Perform an optimum pitch-over into a nearly constant-energy (shallow gamma-angle) dive, if necessary, and accelerate through the transonic region to approximately Mach 1.2, by using turbofan/ATE/ramjet (supercharged afterburner) power
- Execute a long-radius optimum pitch-up to an optimum supersonic climb flight path, by using turbofan/ATE/ramjet power
- Climb to approximately 29 km (95 kft) altitude, and 1890 m/s (6200 ft/s) velocity, at optimum flight path angle and velocity, using proportional fuel flow throttling from turbofan/ATE/ramjet, or full ramjet, as required to maximize total energy acquired per unit mass of fuel consumed as a function of velocity and altitude
- Ignite rocket engines to full required thrust level at 1890 m/s (6200 ft/s) and parallel burn to 2195 m/s (7200 ft/s)
- Shut down airbreather engines while closing airbreather inlet ramps
- Continue rocket power at full thrust

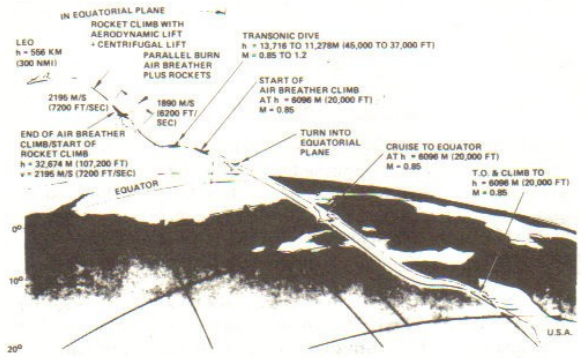

Figure 16. Star-Raker Equatorial Orbit Trajectory

- Insert into an equatorial elliptical orbit 91 x 556 km (50 x 300 nmi) along an optimum lift/drag/thrust flight profile
- Shut down rocket engines and execute a Hohmann transfer to 556 km (300 nmi)
- Circularize Hohmann transfer

The reentry trajectory (shown in Fig. 17) is characterized by low gamma (flight path angle), high alpha (angle of attack) initial atmospheric entry, and aero maneuver descent. The main reentry trajectory elements are:

- Perform delta velocity (ΔV) maneuver and insert into an elliptical orbit 91 x 556 km (50 x 300 nmi)
- Perform a low-gamma, high-alpha deceleration to approximately Mach 20 at an altitude of 82 km (270.000 ft)
- Reduce angle of attack to maximum lift/drag (L/D) for high-velocity glide and crossrange by angle of attack and bank modulation maneuvers to subsonic velocity (approximately Mach 0.85)
- Open inlets and start some airbreather engines
- Perform powered flight to the landing field, land on the runway, and taxi to the dock

Flyback fuel requirements include approximately 300 nmi subsonic cruise and two landing approach maneuvers (first approach waveoff with fly-around second approach).

Required takeoff distances for the Star-Raker were compared with existing data. The distance computed for a tire-rolling coefficient $\mu = 0.10$ agrees with the existing data. Throw weight sensitivity to tire-rolling coefficient is 317 kg (700 lb) (reduction) from $\mu = 0.02$ to 0.20. The data of Fig. 18 show that from 2438 to 3658 m (8000 to 12,000 ft) of takeoff run is reasonable for the current wing-loading, power-loading combination.

The airbreather cruise mode results in an economical orbit plane change from the launch site to the equatorial orbit. Although subsonic cruise takes longer than supersonic cruise, the amount of fuel consumed is substantially less when the orbital plane change is accomplished with subsonic cruise at maximum L/D rather than with supersonic cruise.

Typical ascent trajectory parameters without the cruise leg are shown in Fig. 19. The acceleration load remains less than 2.3 g (76% of Shuttle maximum acceleration), which is a comfortable level for both crew and payload. Maximum dynamic pressure is 60 kPa, which occurs during the airbreather acceleration and is within load limits. From takeoff to burnout, the ascent profile is quite shallow—with flight path angle ranging between -0.7 and 4.5 degrees. Due to the lower AB thrust loading, approximately 75% of flight time is expended during the AB climb/acceleration.

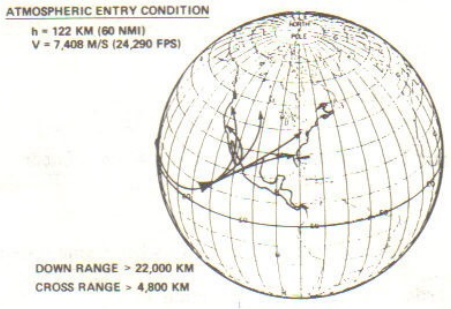

Figure 17. Star-Raker Reentry Trajectories

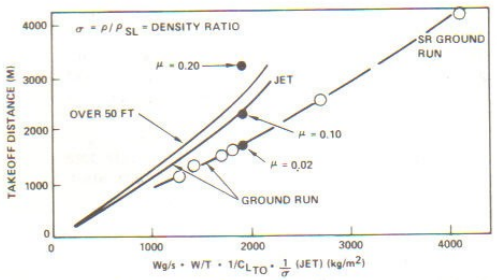

Figure 18. Takeoff Performance

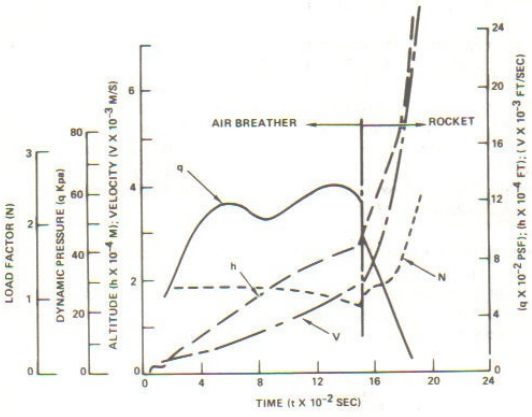

Figure 19. Ascent Trajectory Parameter Histories

A major advantage of the Star-Raker flying-wing vehicle over the VTO ballistic space vehicle is the efficient use of aerodynamic lift during ascent. Since the ballistic system must overcome large gravity losses during lift-off and the ascent period, it requires an initial thrust/weight > 1.0. However, the Star-Raker can have an initial T/Wg < 1 because of the efficient aerodynamic wing with high L/D. This high L/D winged vehicle maintains a shallow flight path angle ($\gamma_e \simeq 2.0^o$) during ascent and permits a greater portion of propulsive energy to be expended in kinetic energy of acceleration and velocity rather than in a gain in potential energy of altitude. This use of energy is more efficient than that of a vertically launched rocket. Furthermore, the additional lift due to centrifugal force becomes available for flight speeds greater than 300 m/s (10,000 ft/s).

Velocity and altitude histories during vehicle ascent vary for different modes of trajectory shaping. However, the ambiguity of performance comparison between different flight trajectories can be eliminated by comparing a plot which shows performance data versus total energy velocity ($V^* = \sqrt{V^2 + 2gh}$), which accounts for potential and kinetic energy variations.

Typical HTO/SSTO performance comparisons of the AB/rocket propulsion and the all-rocket propulsion systems are shown in Figure 20. The difference in throw weight (approximately 186,000 kg ($\Delta W/S = 49$ kg/m^2)) is the cumulative effect of AB engine operation, as compared to the rocket, in the speed regime less than V* = 2000 m/s. Therefore, a net payload increase will result by going from the all-rocket to the AB/rocket system if the additional AB engine system weight requirement is less than the increase in throw weight.

The mass ratio (GLOW/throw weight) is approximately 5, 8, and 20 for the AB/rocket HTO, the all-rocket HTO, and the Space

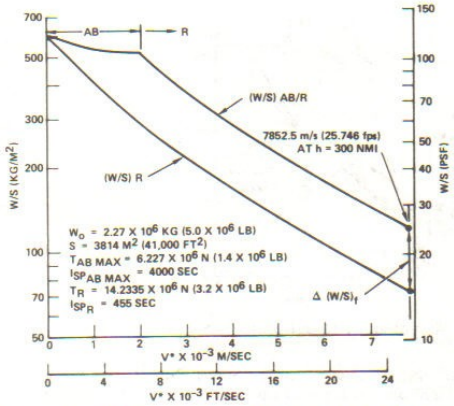

Figure 20. HTO/SSTO Ascent Performance Comparison

Shuttle VTO, respectively. Hence, a well-designed HTO system can improve the throw weight mass ratio over the VTO system.

Weight in orbit is summarized in Table 1. The data entries identified by an asterisk are revised reference vehicle data resulting from Rockwell and NASA/MSFC data exchange in May 1978. Calculations reflect additional fuel reserves, performance losses, and a 10-percent growth factor. Inert weight in orbit was increased from 314,970 kg (694,510 lb) to 352,213 kg (775,800 lb), and airbreather engine thrust of 6.227 x 10^6 N (1.4 x 10^6 lb) constant was revised to reflect increase in the airbreather thrust potential shown in Figure 13.

The lower payload into the equatorial orbit resulted from the expenditure of cruise fuel from the KSC to the equator. The equatorial orbit payload can exceed 90,000 kg if an equatorial based launch site is used. In this case, the Star-Raker without LO_2 weighs less than 707,000 kg (1,300,000 lb) and can fly from the continental United States to the launch site with substantial savings in the cruise fuel.

Ascent and descent trajectories of the Star-Raker and the Space Shuttle missions are compared in Fig. 21. Because the performance of airbreathing engines and aerodynamic lifting of winged vehicle depend on the high dynamic pressure, the Star-Raker flies at much lower altitude during the powered climb

Table 1. Star-Raker Weight in Orbit Summary

Orbit	GLOW W_o x 10^6 kg (W_o x 10^6 lb)	In Orbit W_f x 10^3 kg (W_f x 10^3 lb)	In Orbit P.L. x 10^3 kg (P.L. x 10^3 lb)
Equatorial orbit cruise from KSC	2.27 (5.0)	409.5 (902.0)	57.2 (126.2)
28.5° inclined orbit from KSC due east	2.27 (5.0)	441.5 (972.4)	89.2 (196.6)

- Launch from KSC
- Data for 556.0 km (300 nmi) orbital insertion
- Reference wing area (S_{REF}) = 3814 m^2 (40,900 ft^2)
- Weight in orbit (excluding payload) = 352,213 kg (775,800 lb)*
- Airbreather
  - Thrust = 6.227 x 10^6 N (1.4 x 10^6 lb)
  - I_{SP} = variable
  - Velocity = 0 ≤ V ≤ 1891 m/s (6200 ft/sec)
- Rocket
  - Thrust = 14.23 x 10^6 N (3.2 x 10^6 lb)
  - I_{SP} = see chart
  - Velocity = 1891 m/s (6200 ft/sec ≤ V ≤ V_{orbit}

*W_f = total weight; P.L. = payload

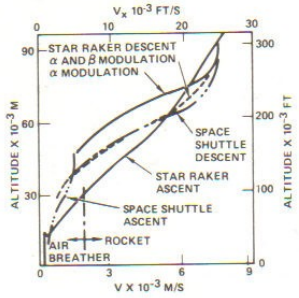

Figure 21. Ascent and Descent Trajectory Comparisons

than the vertical ascent trajectory of the Space Shuttle for a given flight velocity. Light wing loading of the Star-Raker contributes to the rapid deceleration during deorbit.

The total enthalpy flux histories, which indicate the severity of expected aerodynamic heating, are shown in Fig. 22. As expected, the aerodynamic heating of ascent trajectory may determine the Star-Raker TPS requirement. The maximum total enthalpy flux of 68.09 x 10^6 W/m^2 (6000 Btu/ft^2-sec) is estimated near the end of the airbreather power climb trajectory. Except in the vicinity of vehicle nose, wing leading edge, or structural protuberances where interference heating may exist, most of the ascent heating is from the frictional flow heating on the relatively smooth flat surfaces.

The descent heating is mainly produced by the compressive flow on the vehicle windward surface during the high angle-of-attack reentry, and is expected to be considerably lower than the Space Shuttle reentry heating.

Aerodynamic and Structural Heating

Preliminary aerodynamic heating evaluations of the Star-Raker configuration were performed for several wing-spanwise stations and the vehicle centerline.

For the wing lower surfaces, heating rates were computed, including the chordwise variation of local flow properties. Effects of leading edge shock and angle of attack were included in the local flow property evaluation. Leading edge stagnation heating rates were based on the flow conditions normal to the leading edge, neglecting cross-flow effects. All computations were performed using ideal gas thermodynamic properties.

Wing upper-surface heating rates were computed using free-stream flow properties, i.e., neglecting chordwise variations of flow properties. Heating rates were computed for several prescribed wall temperatures as well as the reradiation equilibrium wall temperature condition. Transition from laminar to turbulent flow was taken into account in the computations. Wing/body and inlet interference heating effects were not included in this preliminary analysis. The analysis was limited to the ascent trajectory, since the descent trajectory is thermodynamically less severe.

These parametrically generated aerodynamic heating rate data were used for thermal analysis of the various candidate insulation systems. Radiation equilibrium temperatures for emissivity, $\epsilon = 0.85$, are based on the following:

- Leading-edge stagnation heating rates peak at M = 16.4, altitude = 59,741 m (196,000 ft)
- Upper wing surface temperatures peak at M = 6.4, altitude = 26,365 m (86,500 ft)
- Lower wing surface heating rates and temperatures peak at M = 7.9, altitude = 35,357 m (116,000 ft)

Isotherms of the peak surface temperatures for upper and lower surfaces (excluding engine inlet interference effects) for the Star-Raker are shown in Fig. 23. Star-Raker lower-surface temperatures are from 222°C (400° F) to 333°C (600°F) lower than the orbiter due to lower reentry wing loading, 112 kg/m^2 versus 327 kg/m^2 (23 versus 67 lb/ft^2).

Typical variations of heat leak rate (W/m^2) into propellant filled tanks as a function of HRSI tile thickness for typical upper and lower wing tank locations are shown in Fig. 24. Total heat flux corresponds to a 1500-sec time period during ascent from M = 0.8 at 10,668 m (35,000-ft) altitude.

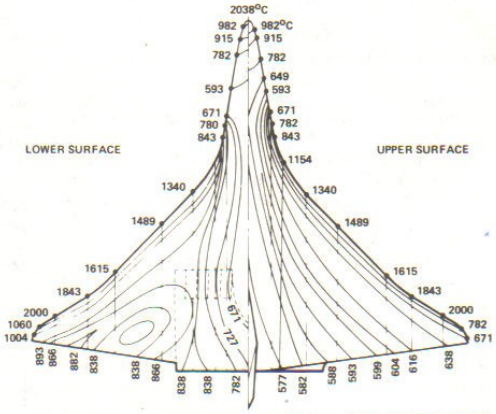

Figure 23. Isotherms of Peak Surface Temperatures During Ascent

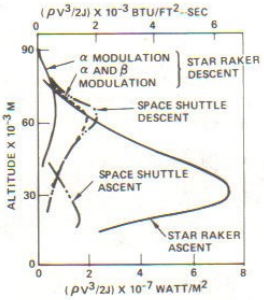

Figure 22. Total Enthalpy Flux Histories

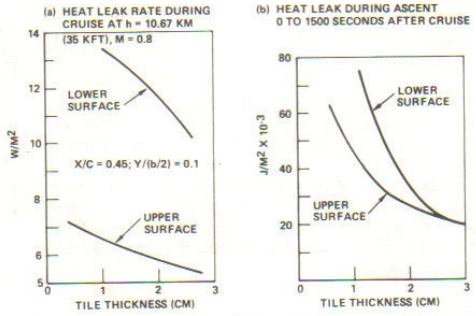

Figure 24. Heat Leak Into Propellant-Filled Wing Tanks

Variation of bondline temperatures versus tile maximum temperature to thickness ratio is shown in Fig. 25. Curve A relates dry tank data for nominal upper surface positions, Curve B shows LH_2 propellant-filled lower surface conditions, and Curve C shows the effects of cold ullage gas in contact with wing upper surface.

Typical thermal response as a function of launch trajectory exposure time of insulation and wing tank structure is summarized in Fig. 26. Part (a) of the figure shows aero heat flux at the HRSI surface and the reradiated component; Part (b) shows tile temperatures from the ceramic surface to the bondline; Part (c) summarizes structure temperatures from the foam bondline to the pressure vessel wall; and Part (d) plots heat flux rate and total flux.

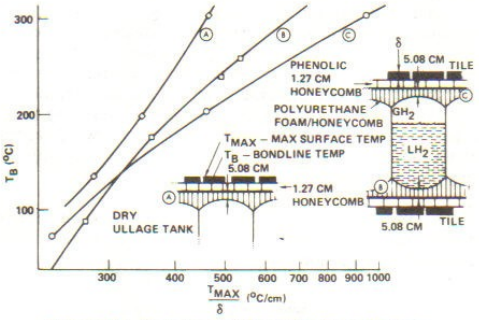

Figure 25. Variation of Bondline Temperature With Tile Thickness

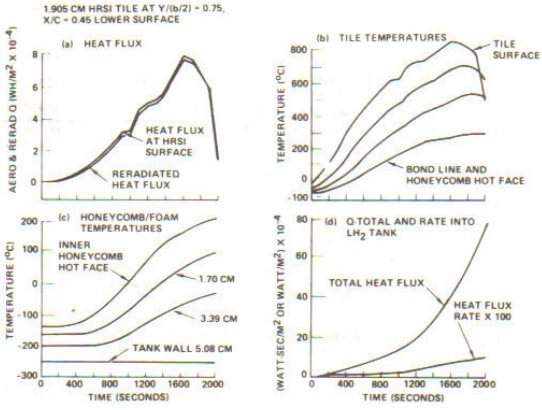

Figure 26. Insulation Thermal Response

Fig. 27 shows HRSI tile thickness profiles for bondline temperatures of 177°C. Preliminary data indicate that the titanium aluminide system described previously may be lighter than the RSI tile for the Star-Raker TPS system due to the low average temperature (538°C to 871°C) profiles occurring over 80% to 85% of the vehicle exterior surface.

Thermal Protection System

Ceramic-coated RSI tile (used on Shuttle) and metallic truss core sandwich structure (developed for the B-1 bomber) were investigated as potential thermal protection systems for Star-Raker (see Fig. 10).

The radiative surface panel consists of a truss core sandwich structure fabricated by a superplastic/diffusion bonding process. For temperatures up to 871°C, the concept utilizes an alloy based

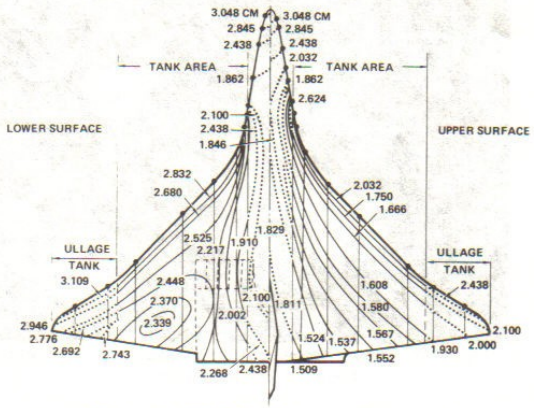

Figure 27. HRSI Tile Thickness Contours for 177°C Bondline Temperature

on the titanium-aluminum systems, which show promise for high-temperature applications currently being developed by the Air Force. For temperatures higher than 871°C, it is anticipated that an alloy will be available from the dispersion-strengthened superalloys currently being developed for use in gas turbine engines. Flexible supports are designed to accommodate longitudinal thermal expansion while retaining sufficient stiffness to transmit surface pressure loads to the primary structure. Also prominent in metallic TPS designs are expansion joints which must absorb longitudinal thermal growth of the radiative surface, and simultaneously prevent the ingress of hot boundary layer gases to the panel interior. The insulation consists of flexible thermal blankets, often encapsulated in foil material to prevent moisture absorption. The insulation protects the primary load-carrying structure from the high external temperature.

During the past two years, Rockwell and Pratt and Whitney Aircraft have participated in an Air Force Materials Laboratory sponsored program, F33615-75-C-1167, directed toward the exploitation of Ti_3Al base alloy systems. The titanium aluminide intermetallic compounds based on the compositions Ti_3Al (α_2) and TiAl (λ), which form the binary Ti-Al alloys, have been shown to have attractive elevated temperature strength and high modulus/density ratios (Fig. 28).

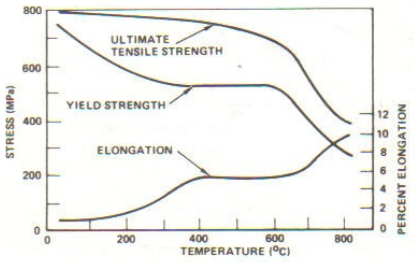

Figure 28. Tensile Properties for Ti-13.5Al-21.5Cb

The titanium hardware depicted in Fig. 29 is an example of complex configurations that have been developed by utilizing a process which combines superplastic forming and diffusion bonding (SPF/DB). This Rockwell proprietary process has profound implications for titanium fabrication technology, per se. In addition, the unprecedented low-cost hardware it generates promises to revolutionize the design of airframe structure. The versatile nature of the process is apparent, showing complex deep-drawn structure and sandwich structure with various core

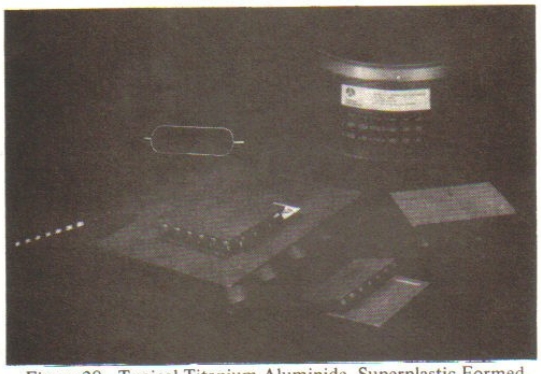

Figure 29. Typical Titanium Aluminide, Superplastic Formed, Diffusion-Bonded Structures

configurations. This manufacturing method and the design freedom it affords offer a solution to the high cost of aircraft structure. Manufacturing feasibility and the cost and weight savings potential of these processes have been established through both IR&D efforts at Rockwell and Air Force contracts. These structures may be used for engine cowling, landing gear doors, etc., in addition to providing major TPS components.

Unit masses of the Star-Raker TPS concept, state-of-the-art TPS hardware, and advanced thermal-structural designs are compared with the unit mass of the orbiter RSI in Fig. 30. The unit mass of the RSI includes the tiles, the strain isolator pad, and the bonding material. The shaded region shown for the RSI mass is indicative of insulation thickness variations necessary to maintain the moldline over the bottom surface of the orbiter. The RSI is required to prevent the primary structure temperature from exceeding 177°C. The unit masses of the metallic TPS are plotted at their corresponding maximum use temperatures. The advanced designs are seen to be competitive with the directly bonded RSI.

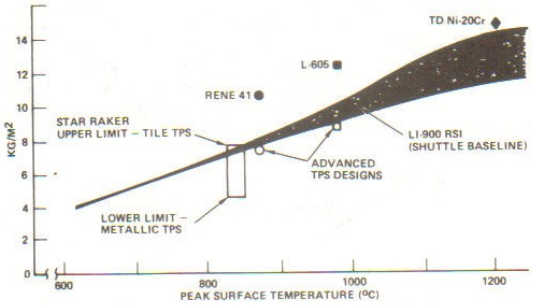

Figure 30. Unit Mass of TPS Designs

Structural Analysis

The multi-cell wing tanks provide a structure which is capable of sustaining pressure while, at the same time, reacting aerodynamic loads. The tanks are sized based on ullage pressures of 221 to 234 kPa, absolute (32 to 34 psia) (LH_2), and 138 to 152 kPa, absolute (20 to 22 psia) (LO_2). Maximum wing-bending occurs at about Mach 1.2. The LH_2 and LO_2 wing tanks are the major load path for reacting these loads. The wing also supports the airbreather engine system.

The primary wing attachment is to the cargo bay structure. The cargo bay aft section, in turn, is connected to the LH_2 tank. The LH_2 tank interconnects the cargo bay, aft portions of the wing, the vertical surface, and the rocket engine thrust structure.

An ultimate factor of safety of 1.50 was used in the analysis. The prime driver in the structural sizing of the multi-cell wing tanks is the bending moment resulting from air loads at Mach 1.2. The net bending moment on the wing is the difference between the lift moment and the relieving moment due to LO_2 remaining in the wing. Trades were performed to determine the structural wing weights required to sustain these bending moments plus internal pressure (Fig. 31). An intermediate location was chosen for LO_2 propellant where lift moment was approximately two times relieving moment. Chordwise location of the LO_2 tank is about the wing c.p. line from the wing root to the wing tip LH_2 ullage tanks. LH_2 tanks are located forward and aft of the LO_2 tanks. A fuel transfer system similar to the British/French Concord maintains propellant c.g. location during launch.

The wing tank was designed to sustain the loads from both internal pressure and wing bending. Al 2219-T87 was chosen for the tank material on the basis of high strength at cryogenic temperatures, fracture toughness, and weldability. Loads resulting from wing bending moments are dominant in determining membrane thickness, which is based on a maximum tank ullage pressure of 234 kPa, absolute, and an ultimate factor of safety of 1.50. Fig. 32 shows material thickness versus wing station due to pressure and wing bending. The column showing bending-only relates to the wing-bending contribution, not an unpressurized wing design.

The fuselage LH_2 tank is the primary load path for reacting total vehicle mass inertias due to rocket thrust during the maximum acceleration condition (3.0 g). Approximately 27% of

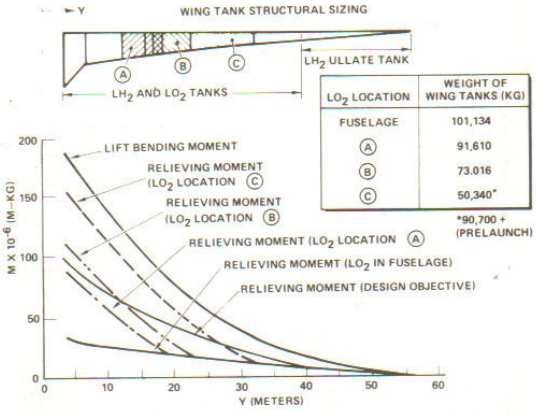

Figure 31. Tank-Relieving Moments Versus LH_2/LO_2 Location

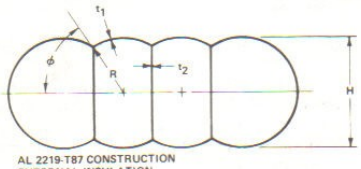

STA* (M)	H_{NOM} (M)	PRESSURE REQUIREMENT $t_1 = t_2$** (MM)	BENDING ONLY t_1 (MM)	BENDING + PRESSURE t_1 (MM)
3.32	6.096	1.676	0.533	2.210
7.01	3.708	1.016	1.016	2.946
16.46	2.794	0.787	2.337	3.124
32.61	1.219	0.356	3.048	3.404

*DISTANCE FROM VEHICLE ℄
**FOR Ø = 60 DEG ONLY

Figure 32. Material Thickness Versus Wing Station

the propellant remains at that time. The tank shown in Fig. 33 has a twin-cone "Siamese" configuration which is required for it to fit in the fuselage at maximum propellant volume. The forward end of the tank is cylindrical, while the aft end is closed out with a double modified-ellipsoidal shell. The bulkheads react the internal pressures whereas the sidewall carries pressure and axial compression loads. The bulkheads are monocoque construction, while the sidewall is an integral skin-stringer with ring frame construction. Tank configuration and bulkhead membrane and sidewall "smeared" thickness requirements to sustain the internal pressure and axial compression loads are reported in Reference 3. The structural design of all cryo tanks is based on cryogenic temperature material properties and allowables.

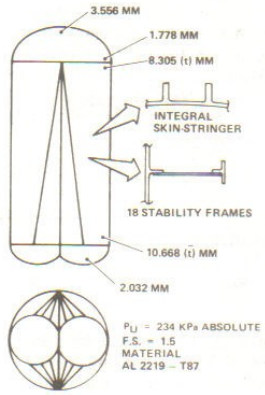

Figure 33. Aft Centerline LH_2 Tank Material Thickness

Mass Properties

Star-Raker mass properties are dominated by the tridelta wing structure, the thermal protection system, and the airbreather and rocket propulsion system. Table 2 is the final reference vehicle weight summary for a due-east 28.5° launch from KSC.

Table 2. Weight Summary, KSC Launch

Item Description	Reference Vehicle (kg)
Airframe, aerosurfaces, tanks, and TPS	167,829
Landing gear	12,565
Rocket propulsion	32,523
Airbreather propulsion	63,503
RCS propulsion	4,536
OMS Propulsion	2,268
Other systems	17,146
Subtotal	300,370
10% growth	30,037
Total inert weight (dry weight)	330,407
Useful load (fluids, reserves, etc.)	21,500
Inert weight and useful load	351,907
Payload weight	89,167
Orbital insertion weight	441,073
Propellant ascent	1,826,890
GLOW (post jettison launch gear)	2,267,960

(557 km), 28.5° inclined orbit

Summary and Conclusions

The combined systems design/performance and technology development studies in CFY 1978 produced a number of significant results.

1. Demonstrated, with end-to-end simulation, the ability of the vehicle to take off from KSC, cruise to the equatorial plane, insert into a 557-km (300-nmi) equatorial orbit with a 57,200-kg (126,200-lb) payload and then to reenter and return to the launch site; also demonstrated the ability to deliver a 89,167-kg (196,580-lb) payload with a due-east launch.

2. Devised a multi-cycle airbreathing engine system concept for operation in turbofan, air-turbo-exchanger, and ramjet modes to provide an effective propulsion match with takeoff, cruise, and acceleration requirements.

3. Showed that Star-Raker lower surface temperatures during reentry are several hundred degrees lower than the lower surface temperatures of the orbiter because of a lower wing loading. As a result, an advanced titanium aluminide system shows promise of being lighter than the RSI tile system for Star-Raker application.

4. Performance was found to scale almost linearly between 453,590 kg (1,000,000 lb) and 2,267,960 kg (5,000,000 lb) GLOW vehicle systems, provided that consistent wing loading and thrust loading are used.

5. Nose loader vehicles can utilize existing cargo-handling techniques used for commercial 747 or military C-5A aircraft systems modified for space at significant weight and cost savings over top-loading vehicles.

6. Aircraft-type operations are significantly more effective and less costly than vertical launch single- or two-stage systems. They have a potential of $22 to $33 per kilogram ($10 to $15 per pound) of payload in orbit.

7. Powered landing capability at any commercial or military airport currently handling 747 or C-5A aircraft.

8. The principal results of the study, which had been performed to an accelerated schedule, were briefed to NASA/MSFC in January 1978; and technical issues resulting from NASA evaluation of the data were essentially resolved by mid-year. Results of the Star-Raker study were utilized in the SPS contract (NAS8-32475). Highlights were included in the SPS final report.[1] Adjusted results were subsequently utilized in the SPS contract extension. As an outgrowth of the Rockwell and NASA/MSFC study and evaluation activities, NASA/MSFC let a contract (NFT-01-002-099), "Airbreathing Engine/Rocket Trajectory Optimization," to the University of Alabama.

9. Suborbital transportation of payloads between point-to-point earth surface launch/landing sites is available commercially as a fallout from space-oriented missions.

10. Key technical areas for further analysis and research are: advanced airbreathing propulsion system; metallic TPS systems; wet-wing tankage and structures analyses; and propellant utilization and c.g. control system analyses.

Appendix

Star-Raker/RASV Comparison (Mini Star-Raker)

Performance trades were developed and comparisons made for (1) a 544,310-kg (1,200,000-lb) version of the Star-Raker with its airbreather/rocket (AB/R) propulsion and (2) the Reusable Aerodynamic Space Vehicle (RASV) with its all-rocket propulsion, as

defined by Boeing.[5] The study was in response to an expression of interest by government agencies who had sponsored the RASV study. The objectives were to determine whether the AB/R configuration could achieve specific performance goals, to identify key operational and performance differences between the AB/R and all-rocket vehicles, and to determine conditions (cross-over) at which performance gains are realized.

Vehicle configurations, major design characteristics, and performance ground rules to permit comparisons of useful payloads are summarized in Fig. 34. The scaled-down AB/R Star-Raker has a tridelta flying wing planform and a Whitcomb airfoil section similar to the Star-Raker designed for the SPS mission. Holding the same gross lift-off weight (GLOW) for the comparison was a study ground rule. The higher empty weight for the scaled down or mini Star-Raker represents the addition of airbreathing engine system and net propellant tank weight increments to the basic RASV weight. As noted, the RASV has a 4536-kg (10,000-lb) payload capability to a 185-km (100-nmi) polar orbit and a 11,340-kg (25,000-lb) capability to a 185-km (100-nmi) orbit at 28°. The payload capability of the mini Star-Raker was to be defined parametrically.

Optimal trajectories for HTO/SSTO concepts, using combined airbreathing rocket (AB/R) and all-rocket propulsion systems were determined as reported in Reference 4. Approximately 1500 seconds of AB operation are required for the AB/R system to reach a transitional velocity ($V_{AB/R}$) of 1830 m/s (6000 ft/s), while 300 seconds are required by the rocket system to reach the same velocity. After $V_{AB/R}$, the time increment required to reach orbital velocity is the same for both vehicles. The corresponding aerodynamic heating parameters, which are proportional to total enthalpy flux histories, were also determined as reported in Reference 4. The data show that the AB/R system will be exposed to a higher heating environment during launch than the all-rocket system because the AB/R system must fly at lower altitudes where the AB engine operates most efficiently.

Total throw weight as a function of launch wing loading and AB/R transitional velocity ($V_{AB/R}$) are also presented in Reference 4. For a given transitional velocity, the throw weight increases rapidly between 4788 and 7182 N/m^2 (100 and 150 lb/ft^2) wing loading, but flattens out between 7182 and 9576 N/m^2 (150 and 200 lb/ft^2). Therefore, considering the substantial increase in the aeroheating parameter between 7182 and 9576 N/m^2 (150 and 200 lb/ft^2), a wing loading of 7182 N/m^2 (150 lb/ft^2) was selected for the rest of the trade studies.

The useful payload capability for the AB/R system, which considers the added weight penalty resulting from AB engines and increased tank weights, is shown parametrically in Fig. 35. For the AB/R configuration, the minimum payload requirement of 4536 kg (10,000 lb) to a polar orbit can be met with a $V_{AB/R}/(T/Wg)_{AB}$ combination of 1220/10, 1372/8, or 1830/6. The payload requirement for 13,608 kg (30,000 lb) into the 28° inclined orbit is also exceeded by these engine performance/weight combinations. Fig. 35 also shows that the payload capability of

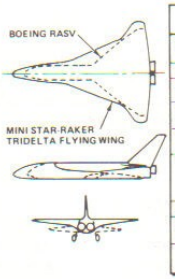

ITEM	MINI STAR-RAKER	RASV (BOEING)
GLOW	0.544 X 10^6 KG + LAUNCHER PROP	0.554 X 10^6 KG + LAUNCHER PROP
W_E (LESS P/L)	91,626 KG (NOM)	63,049 KG
$W_{P/L}$ POLAR:	VARIABLE	4,535 KG
28 DEGREES:	VARIABLE	11,340 KG
WING S_{REF}:	743 M^2	523 M^2
S_{EXP}:	520 M^2	372 M^2
TANK VOLUME LO_2:	276.1 M^3	391.0 M^3
LH_2:	1755.6 M^3	1060.6 M^3
AB ENGINES T_{MAX}:	1,779,290 N	–
$I_{SP_{MAX}}$:	4,000 SEC (FOR ACCEL)	–
LIFT-OFF MODE	HORIZONTAL TAKE-OFF (HTO)	
GROUND-ASSIST TAKE-OFF VELOCITY	–	152 M/S
185 KM (100 NMI) CIRCULAR ORBIT (KSC POLAR AND DUE-EAST LAUNCH IN A 28° INCLINED ORBIT)		

Figure 34. Configuration Characteristics and Ground Rules

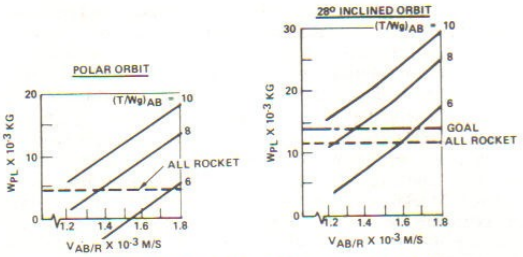

Figure 35. Payload to Orbit Capabilities of Mini Star-Raker and RASV

advanced technology AB engines of Mach 6 and $(T/Wg)_{AB} = 8$ are almost double those of a vehicle with state-of-the-art 177,930-N (40,000-lb) thrust Mach 4 engines ($8 \leq (T/Wg)_{AB} \leq 10$). However, $(T/Wg)_{AB}$ will tend to decrease as $V_{AB/R}$ increases due to the added weight incurred by engine and inlet design complexities resulting from aeroheating effects.

In summary, the performance trade studies for the mini Star-Raker show the following:

1. The mini Star-Raker is capable of placing the desired 4536 and 13,608 kg (10,000 and 30,000 lb) of useful payload into 185.2-km (100-nmi) polar and 28° orbits, respectively.

2. These payload capabilities can be achieved with various combinations of $V_{AB/R}$ ranging from 1219 to 1829 m/s (4000 to 6000 ft/s) and $(T/W)_{AB}$ ranging from 6 to 10.

3. The optimal wing loading is approximately 7182 N/m^2 (150 lb/ft^2) when performance and aeroheating effects are taken into account.

4. The mini Star-Raker is competitive from a performance standpoint with the all-rocket RASV system with moderate advancements in AB propulsion system technology $(T/Wg)_{AB}$ = 8-10, and $V_{AB/R} \simeq 1219$ m/s).

5. The mini Star-Raker offers the potential of major growth in payload capability, e.g., ∿11,340 kg (25,000 lb) into polar orbit and ∿ 22,680 kg (50,000 lb) into 28° orbit, with significant AB propulsion system technology advancement to $V_{AB/R}$ = 1829 m/s (6000 ft/s) and $((T/Wg)_{AB} > 8)$.

6. A major advantage of the AB/R system is operational flexibility. Particularly, the atmospheric cruise capability with AB engines makes this vehicle an excellent air transportation system for ferrying and payload pick-up missions. This capability results in reduced ground and auxiliary air transportation system requirements for logistics support. The mini Star-Raker without LO_2, which is required for space operation only, weighs approximately 136,080 kg (300,000 lb) [W/S ≤ 1915 N/m^2 (40 lb/ft^2)] including the payload and cruise fuel for 6440 km (4000 statute miles). Therefore, the mini Star-Raker can operate in this mode from any airfield which can handle the C-5A or the Boeing 747 and which adds LH_2 facilities.

Acknowledgements

Rockwell personnel including authors who participated in the CFY 1977-1978 IR&D studies are listed below.

G.M. Hanley, Program Manager, Satellite Power System
D.A. Reed, Jr., Responsible Project Engineer
H. Ikawa, Aerothermal and Scientific Adviser

J.P. Sadunas, Aerothermal and TPS
R. Bergeron, Propulsion
J. Collins, Preliminary Design
T. Jasper, Flight Mechanics
C. McBaine, Mass Properties
A. McHugh, Structures
C. Muser, Materials, TPS
P. Ramirez, Propulsion
T. Rudiger, Flight Mechanics THOMAS F
V. Van Camp, Propulsion
R. Wilson, Flight Mechanics

References

1. "Satellite Power Systems (SPS) Concept Definition Study," NAS8-32475 Final Report, Rockwell International, Satellite Systems Division, Report No. SD 78-AP-0023 (April 1978).

2. "Solar Power Satellite Systems Definition Study," NAS9-15196 (1977).

3. D.A. Reed, Jr., "Star-Raker, An Airbreather/Rocket/Powered, Horizontal Takeoff, Tridelta Flying Wing, Single-Stage-to-Orbit Vehicle," Rockwell International, Satellite Systems Division, Report No. SD 78-AP-0044 (November 1978).

4. H. Ikawa, "Preliminary Performance and Sizing Analysis of a HTO/SSTO Vehicle with a 10 to 30 K-lb Payload Capability," Rockwell International, Satellite Systems Division, Report No. SD 78-AP-0104 (November 1978).

5. "Feasibility Study of Reusable Aerodynamic Space Vehicle," SAMSO-TR-76-223, Boeing Aerospace Company (November 1976).

6. "Estimated Performance of a Mach 8.0 Hydrogen Fueled Turbofan Ramjet," Pratt and Whitney Aircraft Report, STFRV-230A (January 1965).

7. "Air-Turborocket Application Study," Aerojet General Corporation (December 1964).

8. "Final Report and User's Manual for the Hypersonic Airbreathing Propulsion Computer Program," NASA Contract NAS2-2985, Rockwell International [North American Aviation], Reports NA66-479 and NA66-530 (May 1966).

9. Virgil K. Smith, "Airbreathing Engine/Rocket Trajectory Optimization Study," University of Alabama (August 1978).

10. Edward S. Rutowski, Douglas Aircraft Company, Inc., "Energy Approach to the General Aircraft Performance Problem," Journal of the Aeronautical Sciences (March 1954).

11. H. Hoeppner, "Dimensionless Flight Mechanics," Rockwell International [North American Aviation, Inc.], Report SID 63-982 (August 1963).

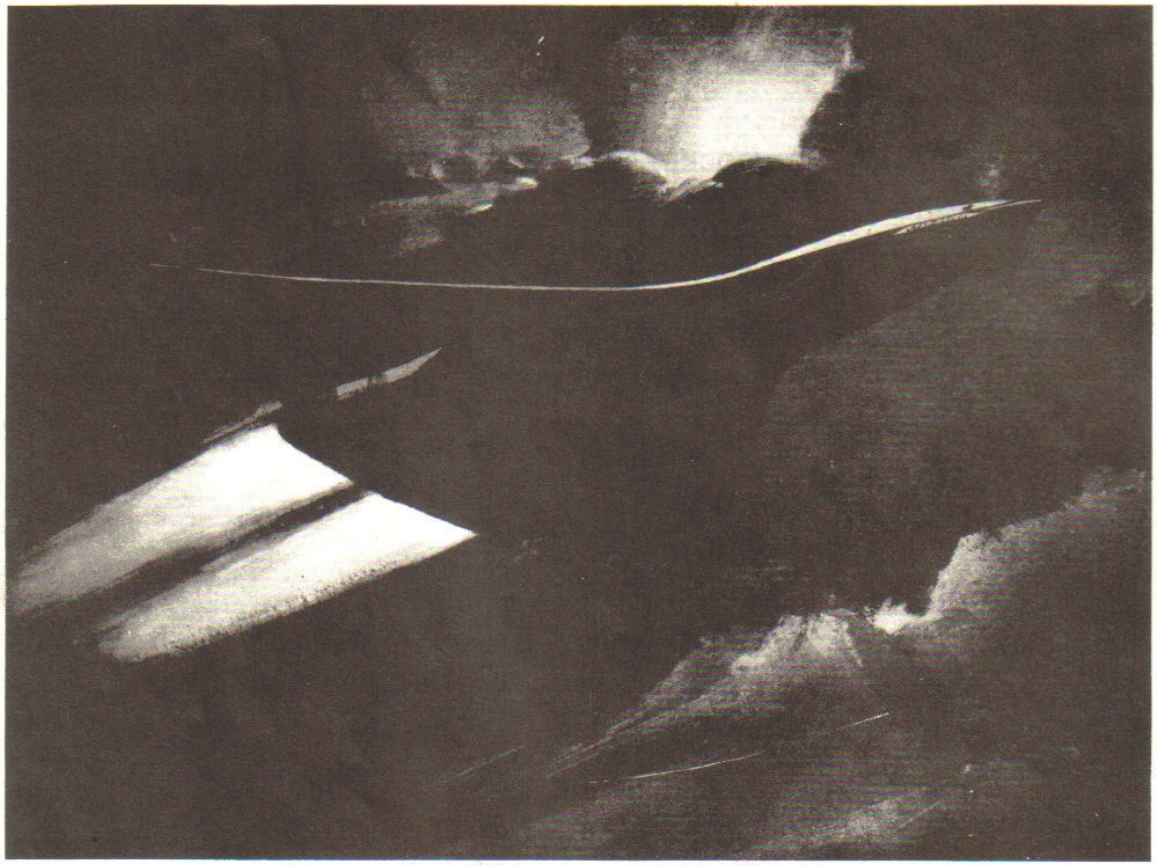

Star-Raker

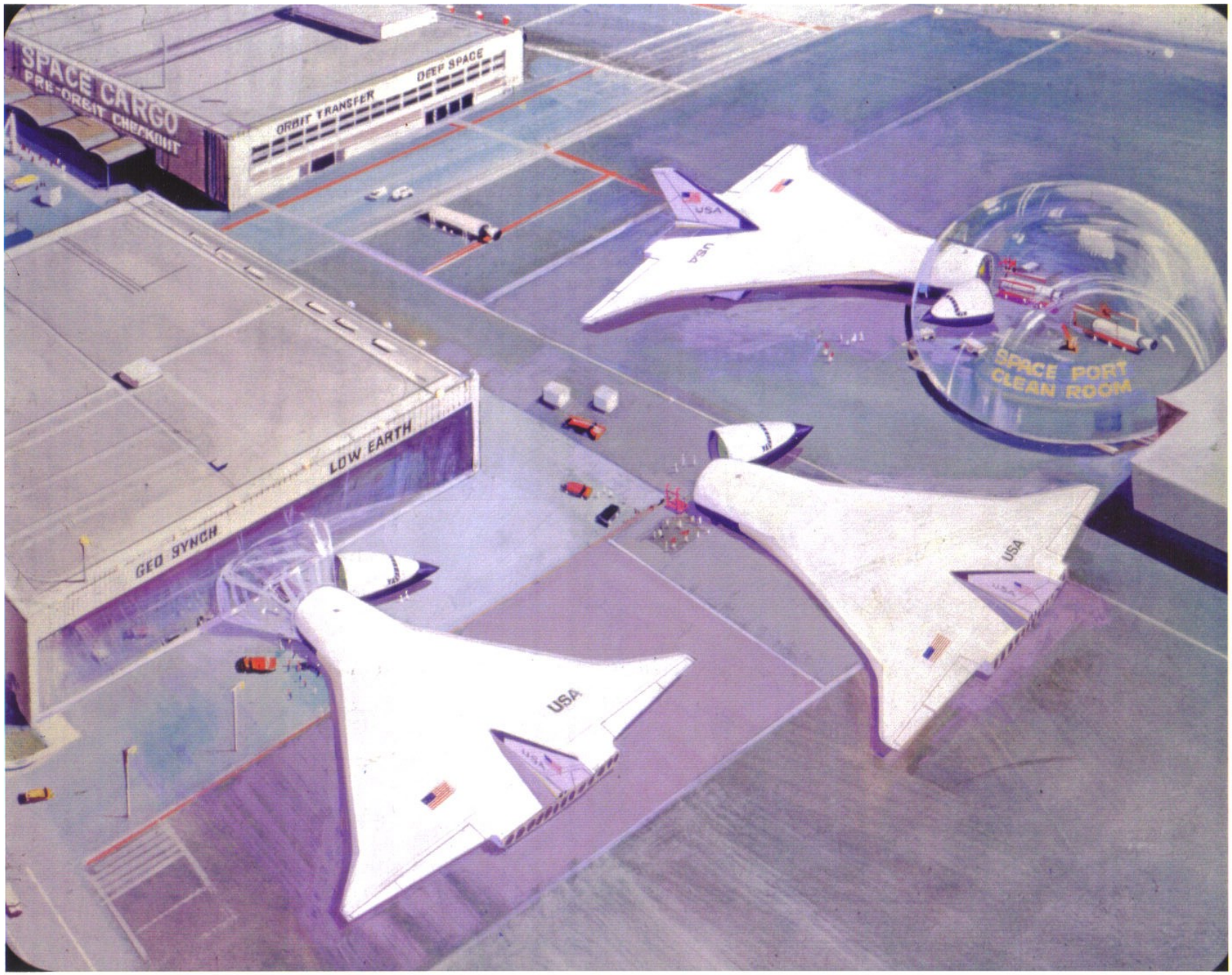
SPACE CARGO
PRE-ORBIT CHECKOUT
ORBIT TRANSFER
DEEP SPACE
LOW EARTH
GEO SYNCH
SPACE PORT
CLEAN ROOM
USA
USA
USA


USA
American

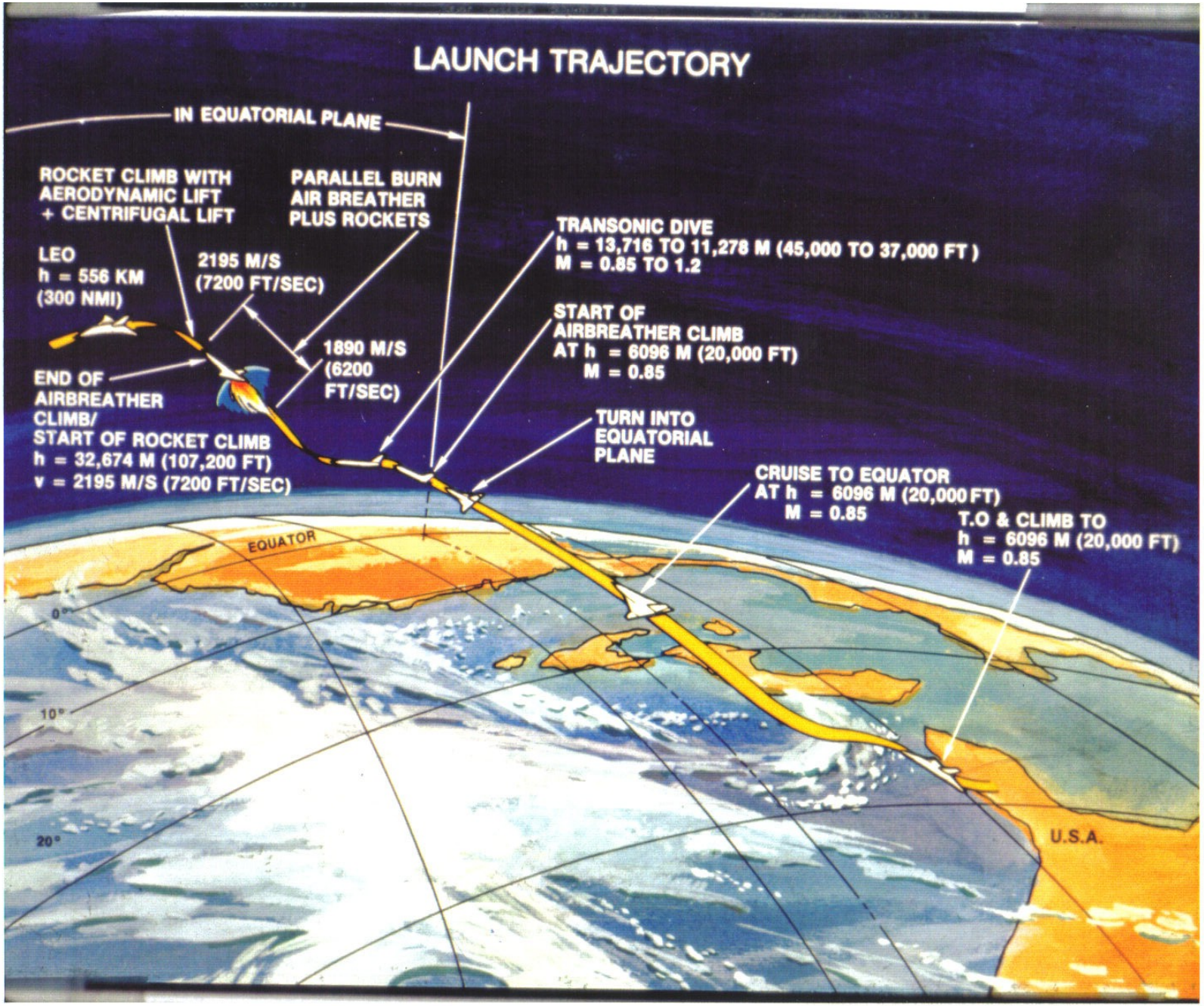
LAUNCH TRAJECTORY
IN EQUATORIAL PLANE
ROCKET CLIMB WITH AERODYNAMIC LIFT + CENTRIFUGAL LIFT
PARALLEL BURN AIR BREATHER PLUS ROCKETS
LEO
h = 556 KM
(300 NMI)
2195 M/S
(7200 FT/SEC)
1890 M/S
(6200
FT/SEC)
END OF AIRBREATHER CLIMB/
START OF ROCKET CLIMB
h = 32,674 M (107,200 FT)
v = 2195 M/S (7200 FT/SEC)
TRANSONIC DIVE
h = 13,716 TO 11,278 M (45,000 TO 37,000 FT)
M = 0.85 TO 1.2
START OF AIRBREATHER CLIMB
AT h = 6096 M (20,000 FT)
M = 0.85
TURN INTO EQUATORIAL PLANE
CRUISE TO EQUATOR
AT h = 6096 M (20,000 FT)
M = 0.85
T.O & CLIMB TO
h = 6096 M (20,000 FT)
M = 0.85
EQUATOR
0°
10°
20°
U.S.A.

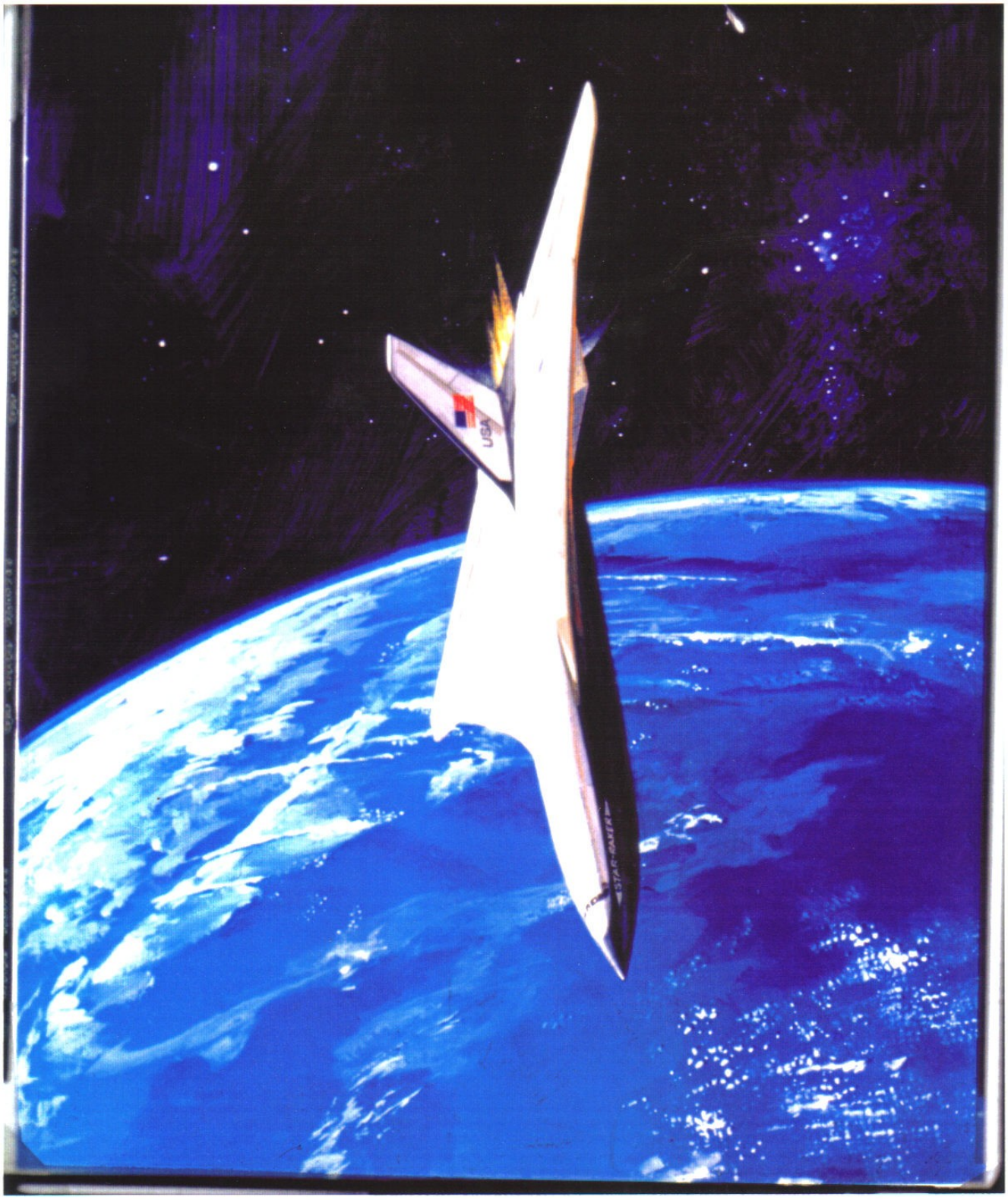
USA

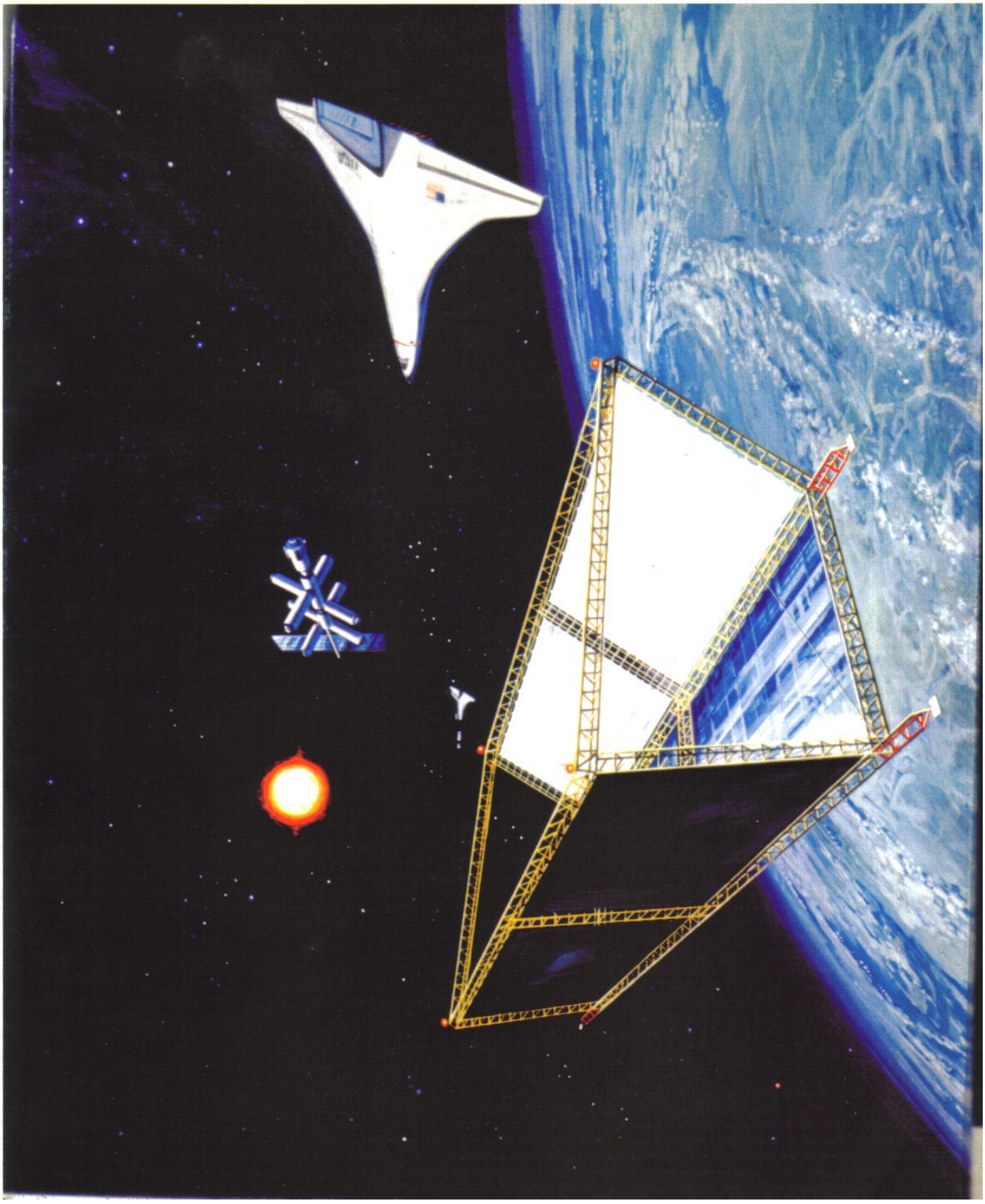


ATMOSPHERIC ENTRY CONDITION
h = 122 KM (60 NMI)
V = 7,408 M/S (24,290 FPS)
DOWN RANGE > 22,000 KM
CROSS RANGE > 4,800 KM

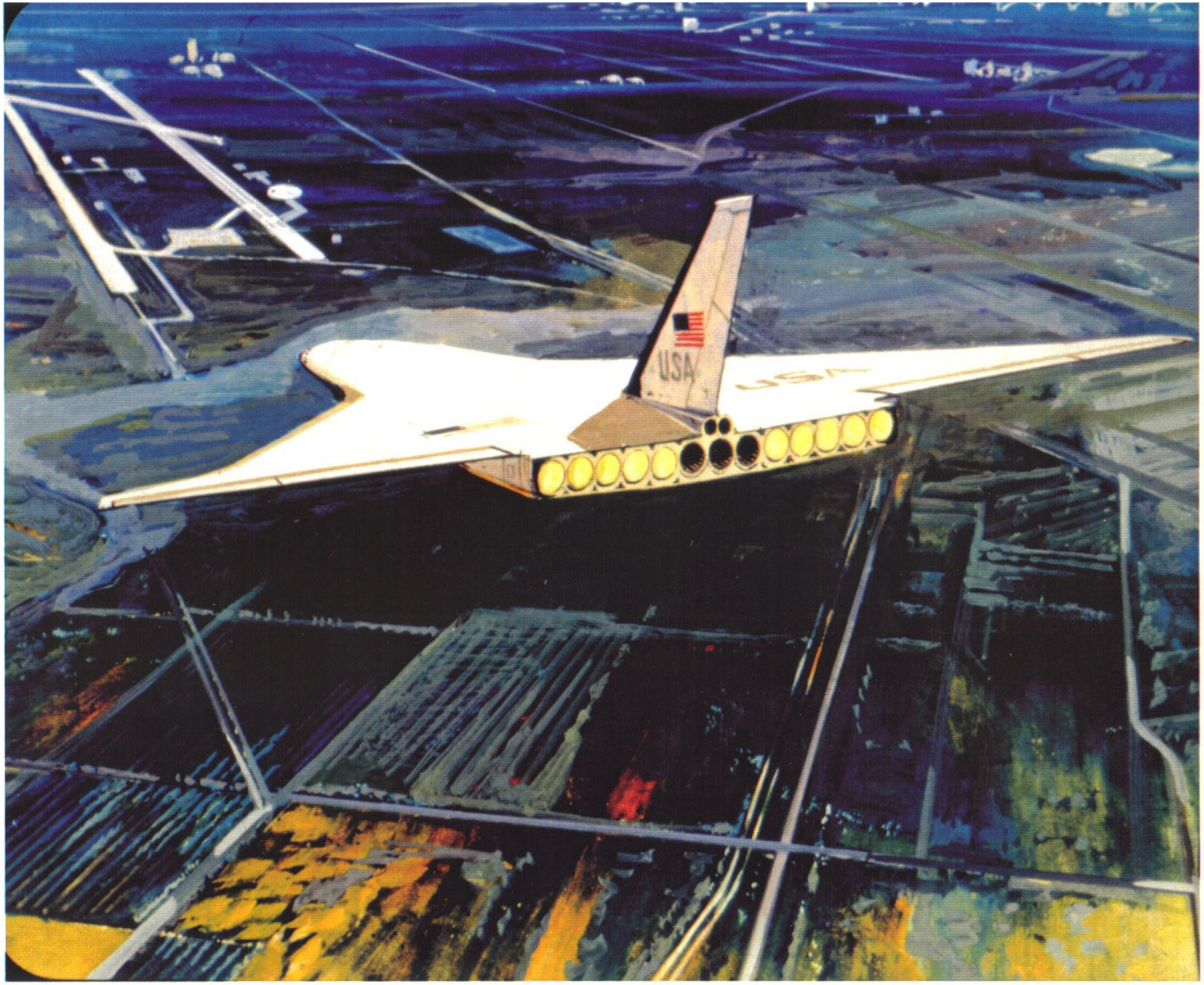
USA

MULTI-CYCLE AIR BREATHING ENGINE
TURBOFAN/AIR TURBOEXCHANGER/RAMJET

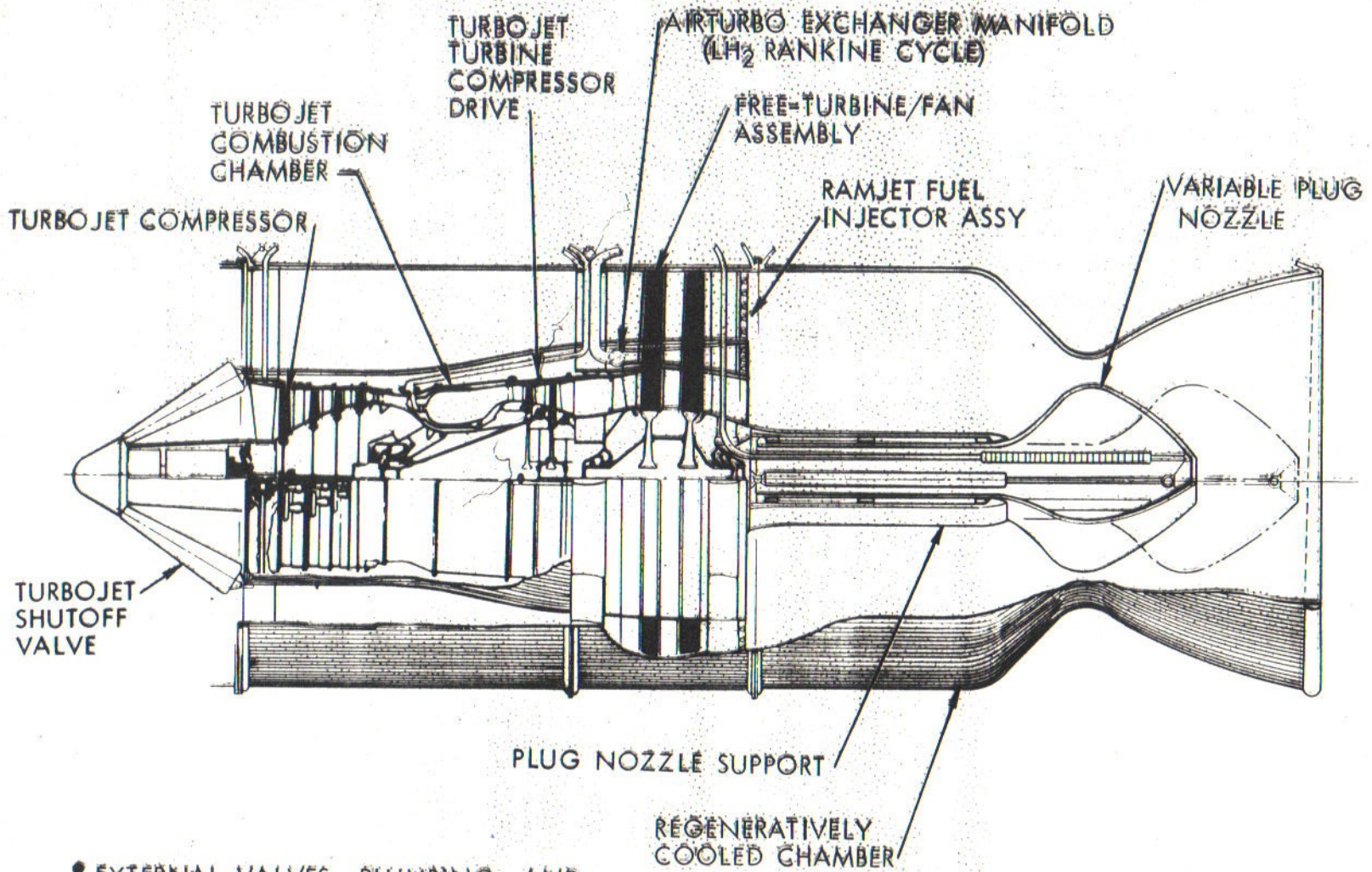

• EXTERNAL VALVES, PLUMBING, AND PUMPS NOT SHOWN

Rockwell International
Space Systems Group

INDEPENDENT RESEARCH AND DEVELOPMENT DATA SHEET	Form Approved. Office Management and Budget Approval No. 22-R 0290

Furnished in confidence and subject to exemption under Subsection(b) of 5 USC 552. The information contained herein is the property of the company indicated in Item 6 below; is furnished for the sole purpose of identifying the subject program and shall not be disclosed other than to duly authorized DoD personnel. Any authorized reproduction or disclosure of the information contained herein, in whole, or in part, shall include this notice.

1. TECH PLAN FY	2. REPORT DATE	3. REPORT TYPE	4. PROJECT NUMBER
- 79	781215	C	243

5. PROJECT TITLE (Unclassified): Earth-to-LEO Transportation System for SPS

6. ORGANIZATION NAME AND ADDRESS:
Rockwell International
Space Systems Group
12214 S. Lakewood Boulevard
Downey, California 90241

7. TECHNICAL PLAN FOCAL POINT NAME: Anderson, N. R.
TELEPHONE: (213) 594-3921

8. PLAN VOL/PG NO.	9. CATEGORY	10. SUBJECT FIELDS AND GROUPS			11. PROJECT START DATE
VII/E-123	S	2202	2101	2004	7710

12. COMPLETION DATE	13. PROFESSIONAL MAN YEARS		SECURITY CLASSIFICATION	
	EST THIS YEAR	CUM TO DATE	14. DATA SHEET	15. REGRADE CODE
7809	0	3.2	U	

16. TECHNICAL CONTACT: Hanley, G. M./D. Reed, Dr. H. Ikawa
TELEPHONE: (213)594-3911

RELATED PROJECTS	17. CURRENT YEAR			18. PREVIOUS YEARS		
	241	206		2641	9531	9341

19. KEYWORDS: Satellite power systems, transportation systems, horizontal takeoff, single stage to orbit, air-breathing engine, performance

20. RELATED DoD TECHNICAL PLANNING & REQUIREMENTS DOCUMENTS & INTERESTED DoD ORGANIZATIONS: JSC (EA7, EA4); MSFC (PD01, PA01, PS01); LaRC (SSD, SST, Aero)

PROJECT FUNDING $K		LABOR	MATERIAL	OTHER	TOTAL
	PRIOR FY 1978	156	0	9	165
	CURRENT FY 1979	0	0	0	0

TECHNICAL PROBLEM

Evolving Satellite Power System (SPS) program concepts envision the assembly and operation of sixty solar-powered satellites in synchronous equatorial orbit over a period of thirty years. Each satellite weighs approximately 81.5 million pounds and is capable of beaming microwave energy to a ground rectenna system which delivers 5 GW at the utility interface. Economic feasibility of the SPS is strongly dependent upon low-cost transportation of SPS elements, interorbital transportation systems, propulsive materials, and operations support equipment between earth and low earth orbit (LEO). The rate of delivery of SPS elements alone to LEO for this projected program is 163 million pounds per year. This translates into 815 flights per year or 2.2 flights per day using a fleet of vehicles, each delivering a cargo of 200,000 pounds.

Earth-to-LEO Transportation System for SPS

The magnitude and sustained nature of this advanced space transportation program concept require long-term routine operations somewhat analogous to commercial airline/airfreight operations. Heavier lift, vertical-takeoff launch vehicles (e.g., 800,000 pound cargo) can reduce the launch rate to 200 or more flights per year. However, requirements such as water recovery of expendable stages with subsequent refurbishment, stacking, launch pad usage, and short turnaround schedules introduce severe problems for routine operations. Studies performed previously showed that substantial operational advantages are offered by an advanced horizontal takeoff, single-stage-to-orbit (HTO-SSTO) aerospace vehicle concept. Further analysis of this concept was needed to provide a promising alternative to heavy lift launch vehicle approaches for LEO logistics support of the SPS, the latter being analyzed as part of an SPS contracted study for NASA/MSFC.

The technical problems needing investigation were of two types: (a) the need for further development of the vehicle system concept including a multicell wet wing containing cryogenic propellants in a blended wing-body configuration; and (b) technology issues, particularly the technical feasibility and performance potential of an advanced hybrid airbreathing engine system, and technical assessment of a flight mode involving horizontal takeoff, long range cruise, subsequent insertion into an equatorial orbit and return via aeromaneuver to the higher-latitude take-off site.

A related technical need, which was addressed briefly, is assessment of the potential of a smaller-scale version of the HTS-SSTO vehicle to deliver cargo to a range of inclinations including polar orbits and to return to the takeoff site, and to meet other DoD-projected requirements.

OBJECTIVE

The general objective of this project is to improve system definition and to advance subsystem technologies for a horizontal takeoff, single-stage-to-orbit vehicle which can provide economical, routine earth-to-LEO transportation in support of a postulated Satellite Power Systems program. Specific objectives for CFY 1978 were:

1. To improve the design definition and technical and operational features of the Star-Raker HTO-SSTO vehicle concept primarily using existing aerodynamic, aerothermal, structural, thermal protection, airbreather and rocket propulsion, flight mechanics and operations technology integrated into a total systems design.

2. To identify disciplines and subsystems in which the application of advanced technology would produce the greatest increase in system performance, and to advance technologies in specific areas.

3. To determine whether a smaller-scale version of the Star-Raker could achieve specific performance goals, and to compare key operational and performance characteristics with an all-rocket propelled vehicle concept.

PROJECT TITLE

Earth-to-LEO Transportation System for SPS

PROJECT SUMMARY

The primary elements of the Star-Raker IR&D study and the related technology issues are summarized in Figure 1. Technical briefings and study progress briefings were given to NASA Headquarters, MSFC, JSC and LaRC, and to USAF/SAMSO. A code showing the general level of government agency acceptance of the study data as being suitable for feasibility confirmation is placed adjacent to technology items. A filled square, ■, indicates concurrence with analytical methods and results. A half-filled square, ◪, indicates data evaluated by NASA MSFC/LaRC that required resolution of differences. The hollow square, □, relates to technology issues not analyzed or which will require detailed in-depth analysis to produce data suitable for feasibility confirmation.

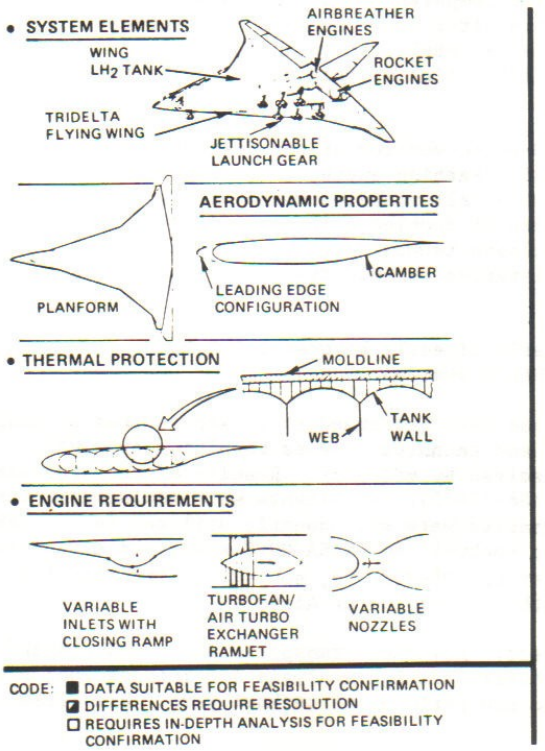

TECHNOLOGY ISSUES (TO PRE-PHASE A TECHNOLOGY LEVEL)

VEHICLE AND SYSTEMS INTEGRATION
PRELIMINARY LAYOUTS OF STRUCTURE
◪ WET-WING ■ CARGO BAY ■ CREW COMPARTMENT
MAJOR SUBSYSTEM INSTALLATION
◪ AIRBREATHER ■ ROCKET ENGINES ◪ GEAR
ENVIRONMENTAL PROTECTION SYSTEM
■ TILE ■ METALLIC TPS ■ INSULATION

REFINE AERODYNAMIC PROPERTIES FOR WAVEDRAG REDUCTION
□ LEADING EDGE CONFIGURATION
■ SPAN THICKNESS DISTRIBUTION
CENTER OF PRESSURE CONTROL
■ TRIDELTA MIX FOR PLAN FORM
□ ENGINE INLET INTERACTIONS

DETERMINE THERMAL PROTECTION SYSTEM
■ AEROTHERMAL ANALYSIS
■ TEMPERATURE PROFILES
■ CANDIDATE TPS SYSTEMS
■ TILE ■ METALLIC

DETERMINE ENGINE REQUIREMENTS
◪ AIRBREATHER ■ ROCKETS
■ INLETS □ NOZZLES
□ MULTIPLE CYCLE ANALYSIS ■ IDENTIFIED
□ AIRBREATHER PERFORMANCE

STRUCTURE ANALYSIS
◪ WING ■ BODY TANK ■ CREW COMPARTMENT
□ CARGO BAY
□ AIRBREATHER ■ ROCKET THRUST STRUCTURE

MASS PROPERTIES ANALYSIS
□ MASS □ CENTER OF GRAVITY

TRAJECTORY ANALYSIS
□ AIRBREATHER ■ ROCKET
■ ENERGY METHOD ■ LaRC POST PROGRAM

Figure 1. Study Summary -- Advanced Transportation System for SPS

The combined systems design/performance and technology development studies in CFY 1978 produced a number of significant results.

1. Demonstrated, with end-to-end simulation, the ability of the vehicle to take off from KSC, cruise to the equatorial plane, insert into a 300 nmi equatorial orbit with 151,000-pound payload, and then to re-enter and return to the launch site; also to deliver a 196,000-pound payload with a due-East launch.

2. Devised a modified airbreathing engine cycle for operation in turbofan, air-turbo-exchanger and ramjet modes to provide an effective match with takeoff, cruise and acceleration requirements.

3. Showed that Star-Raker lower surface temperatures during re-entry are several hundred degrees lower than orbiter lower surface temperatures because of a lower wing loading. As a result, an advanced titanium aluminide system shows promise of being lighter than the RSI tile for Star-Raker application.

4. Performance trades for a 1,200,000-pound version of the Star-Raker based on moderate advancement in airbreathing engine technology showed competitive performance with an all-rocket-powered vehicle. Payload lift capabilities to LEO can be doubled with significant advancements in airbreathing propulsion technology, e.g., engine thrust-weight ratio of 8 and acceleration to 6000 fps prior to rocket transition.

5. Performance was found to scale nearly linearly between 1,000,000-pound and 5,000,000-pound GLOW vehicle systems.

The principal results of the study, which had been performed to an accelerated schedule, were briefed to NASA/MSFC in January 1978, and technical issues resulting from NASA evaluation of the data were essentially resolved by mid-year. Results of the Star-Raker study were utilized in the SPS contract (NAS8-32475). Highlights were included in the SPS final report, Reference 1. Adjusted results were subsequently utilized in the SPS contract extension. As an outgrowth of the Rockwell and NASA/MSFC study and evaluation activities, NASA/MSFC let a contract, number NFT-01-002-099, subject: "Airbreathing Engine/Rocket Trajectory Optimization" to the University of Alabama.

Of the five tasks which comprised the project, "Advanced Transportation - STS Launch" was a systems-oriented activity, which emphasized design analysis and integration; and four supporting tasks emphasized propulsion and performance technologies. All tasks were completed in CFY 1978.

TASK TITLE	CFY 1978 TASK NO.
Advanced Transportation - SPS Launch	26410
Airbreathing Launch Vehicle Engine Systems	95320
Aerodynamic Characteristics Predictions	93420
HTO Airbreathing Launch Vehicle Performance	91120
Orbit Determination and Error Analysis	91430

CFY 1979 APPROACH

This is a completed project. Further Advanced Space Transportation studies are being performed in Project 206.

PROGRESS IN CFY 1978

More than 90 percent of the study was directed to defining and refining design and performance, and resolving technical issues regarding the basic Star-Raker concept for support of a Satellite Power Systems program. Basic requirements for logistics support in the form of transportation of cargo between the earth and low earth orbit (LEO) were generated in the SPS contracted activities, Reference 1. Goals for the Star-Raker concept which are additive to the quantitative requirements for logistic support of the SPS include both NASA and SAMSO objectives/requirements.

- Total vehicle reusability - with many reuses
- Rapid turnaround
- Ferry capability with cargo between airfields
- Minimized launch costs
- High reliability of delivery
- Ability to reach any LEO plane from alternate launch sites (KSC, VAFB and others) and return to the same site; includes single-pass orbits
- Cargo security

Less than 10 percent of the study effort was directed to the preliminary definition of a smaller-scale (1,200,000-pound) version of the Star-Raker and comparison with an all-rocket vehicle of the same weight from a SAMSO-sponsored study.

Study results are presented by subject, as follows, rather than by task to simplify the review process.

- Operational features
- Design features
- Multicycle airbreather engine system
- Aerodynamic characteristics
- Flight mechanics
- Aerodynamic and structural heating
- Thermal protection system
- Structural analysis
- Mass properties
- Orbit determination
- 1,200,000-lb Star-Raker/RASV comparison

OPERATIONAL FEATURES

The Star-Raker concept adapts existing and advanced commercial and/or military air transport system concepts, operations methods, maintenance procedures, and cargo handling equipment to include a space-related environment. The principal operational objective was to provide economic, reliable transportation of large quantities of material between earth and LEO at high flight frequencies with routine logistics operations and minimal environmental impact. An associated operational objective was to reduce the number of operations required to transport material and equipment from their place of manufacture on earth to low earth orbit.

Operations features derived in the study are as follows:

- Single orbit up/down to/from the same launch site (at any launch azimuth subject to payload/launch azimuth match)
- Capable of obtaining 300 nmi equatorial orbit launched from KSC
- Takeoff and land on 8,000 to 14,000-foot runways (launch velocity $\simeq$ 225 knots; landing velocity $\leq$ 115 knots)
- Simultaneous multiple launch
- Total system recovery including takeoff gear jettisoned and recovered at launch site

- Aerodynamic flight capability from payload manufacturing site to launch site, addition of launch gear and fueling, and launch into earth orbit
- Amenable to alternative launch/landing sites
- Incorporates Air Force (C-5A Galaxy) and commercial (747 cargo) payload handling, including railroad, truck, and cargo-ship containerization concepts, modified to meet space environment requirements
- Swing-nose loading/unloading, permitting normal aircraft loading-door facility concept application
- Propulsion system service using existing support equipment on runway aprons or near service hangars
- In-flight refueling options (option not included in reference vehicle data)

Figure 2 shows a Star-Raker vehicle in an airport environment alongside a Boeing 747 passenger transport.

DESIGN FEATURES

The star-Raker utilizes a tri-delta flying wing, consisting of a multi-cell pressure vessel of tapered, intersecting cones. The tri-delta planform (blended fuselage-wing) and a Whitcomb airfoil section offer an efficient aerodynamic shape from a performance standpoint and high propellant volumetric efficiency. The outer panels of the wing and vent system lines in the wing's leading edge provide the gaseous ullage space for LH_2 fuel. LH_2 and LO_2 tanks are located in each wing near the vehicle c.g., and extend from the root rib to the wing tip LH_2 ullage tank (see Figure 3). Approximately 20% of the volume of the vertical stabilizer is utilized as part of the gaseous ullage volume of the integral wing-mounted LO_2 tanks. In the aft end of the vehicle, three uprated high-P_c rocket engines (thrust = 3.2×10^6 lb) are attached with a double-cone thrust structure to a two-cell LH_2 tank.

Most of the cargo bay side walls are provided by the root-rib bulkhead of the LH_2 wing tank. The cargo bay floor is designed similar to the C5-A military transport aircraft. This permits the use of MATS and Airlog cargo loading and retention systems. The top of the cargo bay is a mold-line extension of the wing upper contours, wherein the frame inner caps are arched to resist pressure at minimum weight. The forward end of the cargo bay has a circular seal/docking provision to the forebody. Cargo is deployed in orbit by swinging the forebody to 90 or more degrees about a vertical axis at the side of the seal, and transferring cargo from the bay into space or to in-space receivers on telescoping rails.

The forebody is an RM-10 ogive of revolution with an aft dome closure. The ogive is divided horizontally into two levels. The upper level provides seating for crew and passengers, as well as the flight deck. The lower compartment contains electronic, life support, power (fuel cell), and other subsystems including spare life support and emergency recovery equipment.

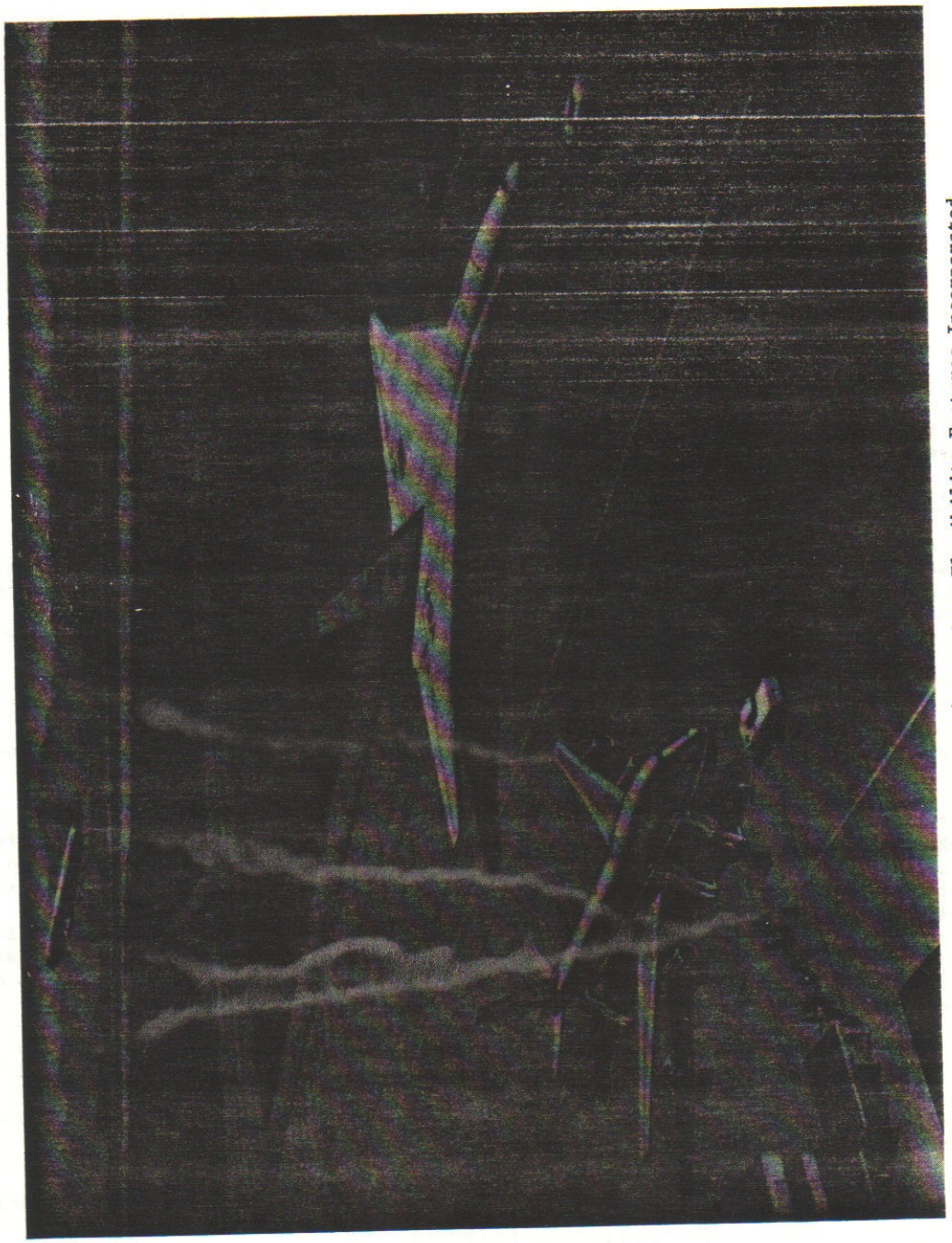

Figure 2. Conventional/Operations Flexibility Features Incorporated in Star-Raker Concept

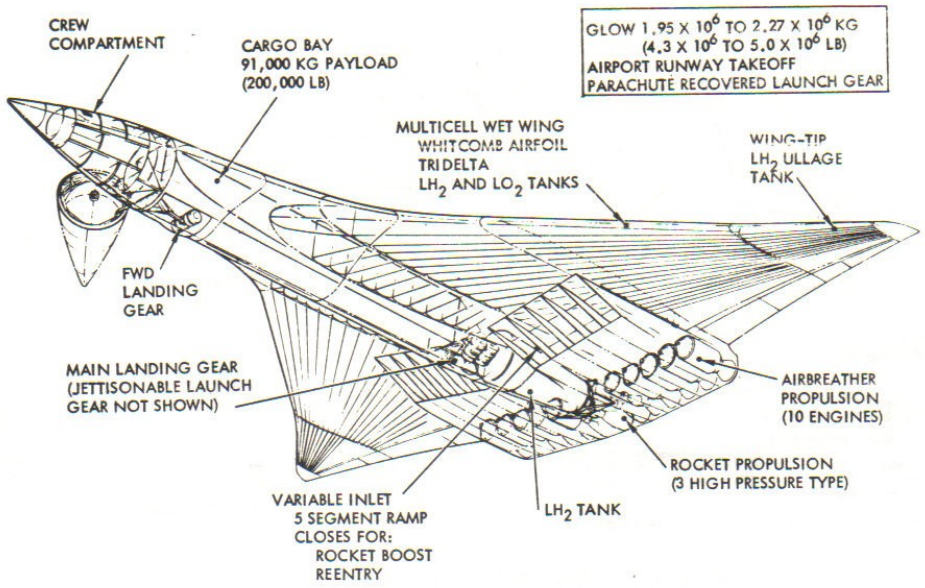

Figure 3. Star-Raker Design Features

Ten high-bypass, supersonic-turbofan/airturbo-exchanger/ramjet airbreather engines with a combined static thrust of 1.4×10^6 lb are mounted under the wing. The inlets are variable area retractable ramps that also close and fair the bottom into a smooth surface during rocket powered flight and for either Sanger skip glider or high angle-of-attack ballistic re-entry.

Figure 4 shows an inboard profile of the vehicle, illustrating the details of body construction, crew compartment, cargo bay length, LH_2 tank configuration, and location of the rocket engines at rear of fuselage. The hinging and rotation of the nose section for loading and unloading the payloads are illustrated, with indication of view angle from the rear of the nose section during these operations. The multiple landing gear concept shows the position of the nose gear bogie, the jettisonable takeoff gear, and the main landing gear for powered landing.

Figure 5 presents front and rear views of the vehicle showing the blended wing, engine inlet ducts, landing gear arrangement, and vertical stabilizer. Also shown are typical sections through the vehicle at:

- The hinge line section (B-B) aft of the crew compartment and forward of the nose gear. Cross-sectional dimensions of the cargo bar are indicated.

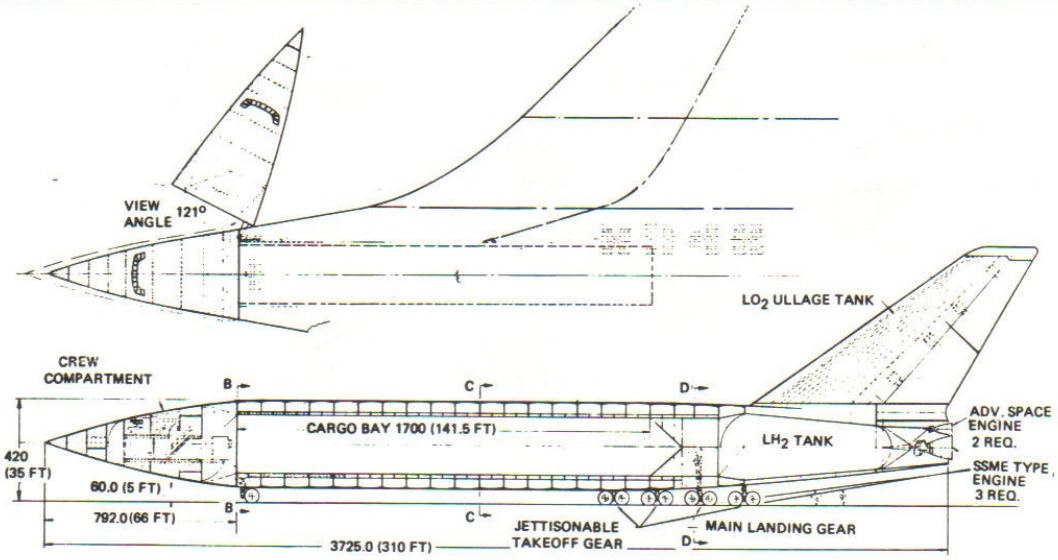

Figure 4. Star-Raker Inboard Profile

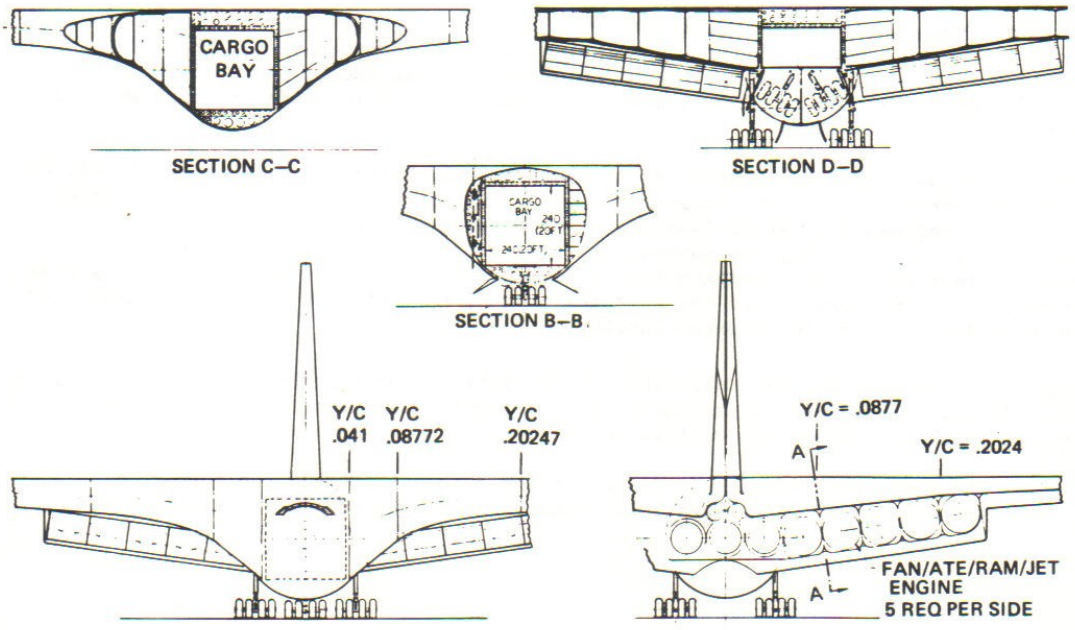

Figure 5. Vehicle Section Results

- The 40% chord line fuselage section (C-C) illustrating the wing and fuselage construction and the profile of the wing/fuselage fairing.
- The main landing gear station (D-D) illustrating the gear retraction geometry, the relationship of the gear to the engine air inlet ducts and the wing construction and profile to the fuselage shape.

Figure 6 presents details of the basic multi-cell structure of the Star-Raker wing. The upper portion illustrates the application of "Shuttle-type" RSI tile thermal protection system (TPS). The lower portion shows a potential utilization of a "metallic" TPS.

The wing is an integrated structural system consisting of an inner multi-cell pressure vessel, a foam-filled structural core, an inner facing sheet, a perforated structural honeycomb core, and an outer facing sheet. The inner multi-cell pressure vessel arched shell and webs are configured to resist pressure. The pressure vessel and the two facing sheets, which are structurally interconnected with phenolic-impregnated, glass fiber, honeycomb core, resist wing spanwise and chordwise bending moments. Cell webs react winglift shear forces. Torsion is reacted by the pressure vessel and the two facing sheets as a multi-box wing structure.

The outer honeycomb core is perforated and partitioned to provide a controlled passage, purge and gas leak detection system function in addition to the function of structural interconnect of the inner and outer facing sheets. The construction of the wing structure utilizes the "Inflation Assembly Technique" developed by Rockwell for the Saturn II booster common bulkhead.

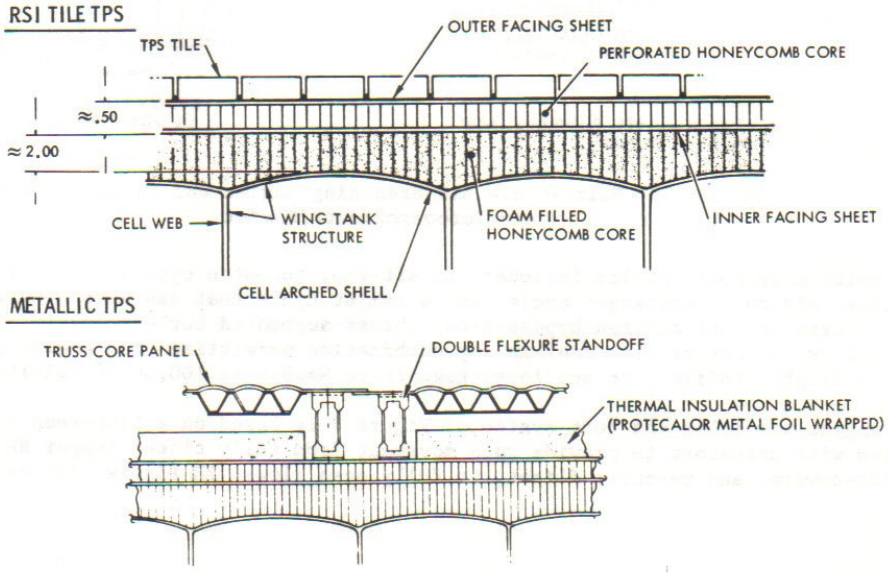

Figure 6. Wing Construction Detail With Candidate TPS Configurations

MULTI-CYCLE AIRBREATHER ENGINE SYSTEM

Takeoff and climb to 100,000 ft altitude and 5,800 fps is by airbreather propulsion. Parallel burn of airbreather and rocket propulsion occurs between 5,800 to 7,200 fps. Rocket power propels Star-Raker from 7,200 fps into orbit.

The multi-cycle airbreathing engine system, Figure 7 is derived from the General Electric CJ805 aircraft engine, the Pratt and Whitney SWAT 201 supersonic wrap-around turbofan/ramjet engine, the Aerojet Air Turborocket, Marquardt variable plug-nozzle, ramjet engine technology, and Rocketdyne tubular-cooled, high-P_C rocket engine technology.

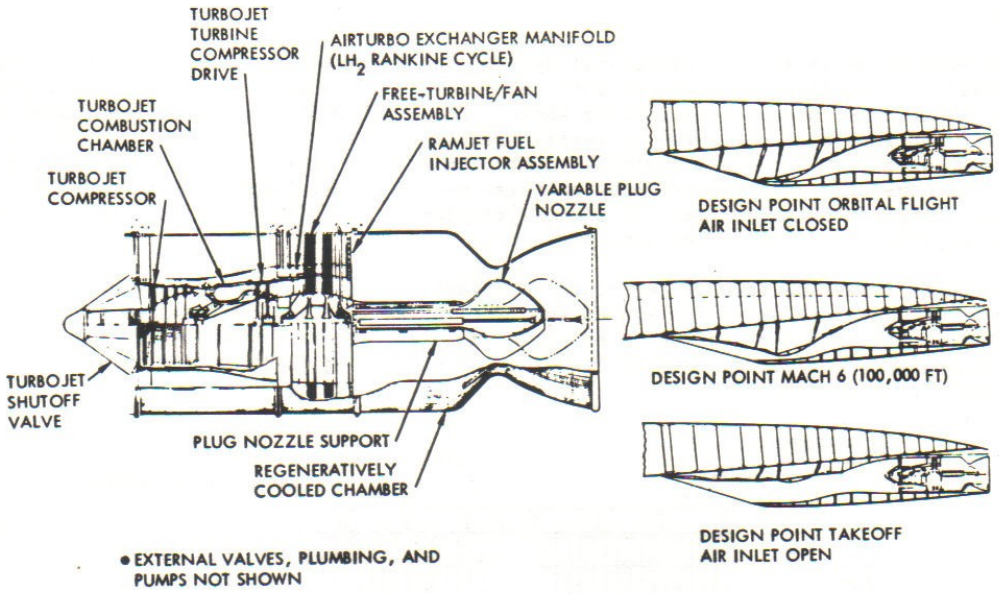

Figure 7. Multi-Cycle Air Breathing Engine and Inlet, Turbofan/ Air Turboexchanger/Ramjet

The multi-mode power cycles include: an aft-fan, turbofan cycle; a LH_2, regenerative Rankine, air-turbo-exchanger cycle; and a ramjet cycle that can also be used as a full flow (turbojet core and fan bypass flow) thrust-augmented turbofan cycle. These four thermal cycles may receive fuel in any combination permitting high engine performance over a flight profile from sea level takeoff to Mach 6 at 100,000 ft altitude.

The engine air inlet and duct system of Figure 7 is based on a five-ramp variable inlet system with actuators to provide ramp movement from fully closed (upper RH figure) for rocket-powered and re-entry flight, to fully open (lower RH figure) for takeoff operation.

The inlet area was determined by the engine airflow required at the Mach 6 design point. The configuration required 1.4 x 10^6 pounds thrust at the Mach 6 condition and at least 1.2 x 10^6 pounds for takeoff. This resulted in an inlet area of approximately 1200 ft^2 or 120 ft^2/engine for a 10-engine configuration. In order to provide pressure recovery with minimum spillage drag over the wide range of Mach numbers, a variable multi-ramp inlet is required. Inlet pressure recovery efficieny vs. velocity is plotted on Figure 8. Higher recoveries are possible for the HTO vehicle than for military aircraft which must operate during more violent maneuvers. However, the pressure recovery must still provide a margin which prevents inlet instability and possible engine flameout from expulsion of the normal shock during transients.

Estimated engine thrust (total of 10 engines) versus velocity is plotted on Figure 9. Initially, a constant thrust of 1.4 million pounds of thrust was assumed for the Rockwell modified Rutowski energy method trajectory analysis (dashed curve of Figure 9). A tentative airbreather engine performance map was estimated from engine data sources previously described. Coordination between Rockwell and NASA/MSFC team members produced the engine thrust versus Mach number estimate shown by the upper solid curve of Figure 9.

All major engine companies were contacted to obtain assistance in advanced cycle analysis and to obtain the results of any studies which investigated this operating regime. Data from a Pratt and Whitney report (Reference 2) on an advanced hydrogen burning engine, the SWAT 201 turbofan ramjet, were evaluated and scaled up to the size required. However, this engine, which uses a bypass valve to close off the engine core above Mach 3.1 and operates the afterburner as a ramjet at higher speeds, did not provide a good match of thrust requirements over the required operating range. Also because of the high compression-ratio design, the engine thrust-to-weight ratio (T/W) was in the range of 4.5 to 5.5 for an installed system. Single-stage-to-orbit launch vehicle analysis showed that a T/W of at least 8 would be necessary to meet the vehicle payload requirements. From Aerojet, (Reference 3) data were obtained on an air turborocket concept which provides a potential for meeting the required T/W values while providing a better match of

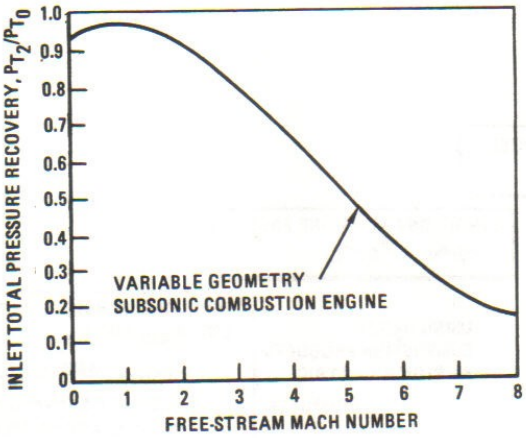

Figure 8. Air Induction System Performance

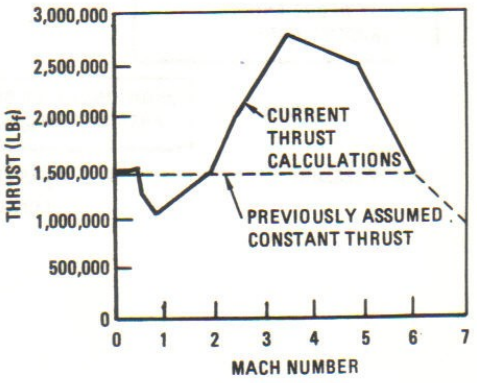

Figure 9. Air Breather Thrust Versus Mach Number

thrust required at takeoff, transonic and supersonic conditions. A modification of this cycle was devised by Rockwell to best match the SSTO requirements. This engine operates as an augmented turbofan for takeoff, a turbofan for high-efficiency cruise, an augmented turbofan for acceleration, and as a ramjet above Mach 3.

The engine components include a rotary vane assembly to close off the compressor-turbine assembly at higher mach numbers. The use of LH_2 fuel permits the use of a Rankine-cycle air turbo-exchanger concept to provide power for the bypass fan. This allows elimination of approximately one-half of the normal turbofan compressor stages normally needed for fan drive. Heating of the LH_2 in outer walls and nozzle plug of tubular construction, in addition to providing fan drive power, permits stoichiometric combustion in the augmentor/ramjet by cooling of exposed surfaces. The 5500-degree combustion temperature provides high cycle efficiency. During ramjet mode operation, the fan is allowed to windmill and is cooled by flow of LH_2 through the fan guide vanes.

The study scope did not permit a detailed evaluation of engine components to provide further, more accurate calculation of the performance capability of this engine concept. Engine manufacturers are best equipped to further refine the design and provide real data on concept feasibility and system weight. The engine companies contacted were not interested in further work without government funding.

For preliminary estimation of airbreathing propulsion system size requirement, a computer program was developed for the Hewlett Packard computer. A flow diagram of this program is shown in Figure 10.

A computer program which has the capability of computing performance of mixed-cycle engines including JP and LH_2 fuel, as well as the air turbo exchanger cycle was obtained from the Los Angeles Division of Rockwell (Reference 4). This program was developed under NASA contract in 1966 and is currently used by LAD for calculation of JP-fueled turbojet and turbofan engine data for advanced aircraft.

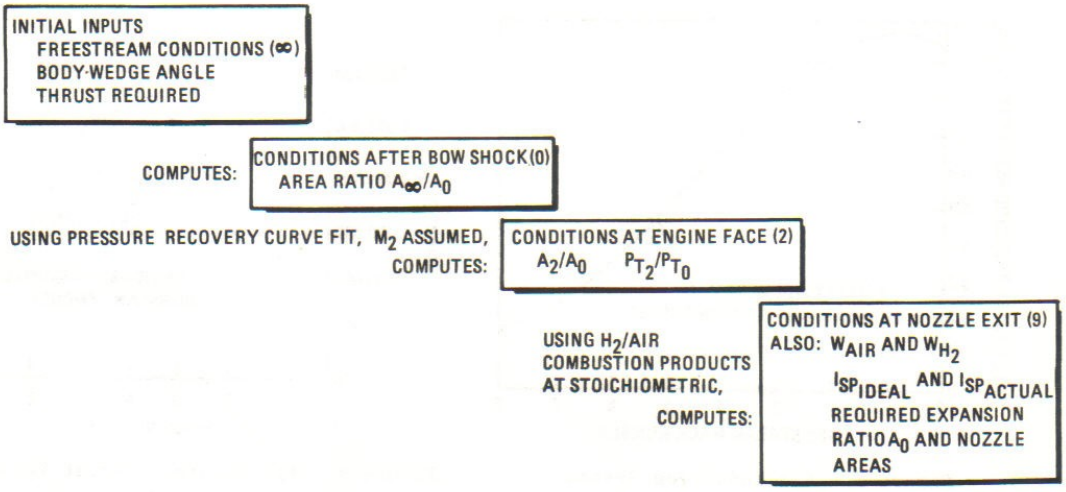

Figure 10. Computer Program Flow Diagram for Air Breather Propulsion System Sizing

In order to maximize the payload boosted to orbit, an optimization technique is required to define the proper engine sequencing over the flight trajectory. Research at NASA/MSFC and Rockwell has focused on improving the mathematical models of the airbreathing propulsion systems, which can be mated with the rocket engine model and incorporated in trajectory optimization codes. As a result of the NASA/MSFC and Rockwell findings, NASA/MSFC let a contract, number NFT-01-002-099, AIRBREATHING ENGINE/ROCKET TRAJECTORY OPTIMIZATION, with the University of Alabama (Reference 5). Program description documents and users manuals for the mixed cycle propulsion computer program were provided to NASA Marshall Space Flight Center for inclusion in that study.

AERODYNAMIC CHARACTERISTICS

The selected wing shape is a supercritical Whitcomb airfoil with a relatively blunt leading edge, flat upper surfaces and cambered trailing edges. The trailing-edge camber and the tri-delta shape minimize translation of the center of pressure throughout the flight Mach number regime. The blunt leading edge offers good subsonic characteristics, but produces relatively high supersonic wave drag; therefore, further shape and refinements are recommended. The wing has a spanwise thickness distribution of 10 percent at the root, 6 percent near midspan, and 5 percent at the tip, providing a large interior volume for storage of LH_2 fuel.

Aerodynamic coefficients (C_L, C_D, C.P.) were calculated using the Flexible Unified Distributed Panel program FA-475, which was developed by the LAD Aerodynamic group. Because the governing equation is linear, singular behavior of the linear equation and nonlinearity near M = 1.0 preclude the transonic solutions. Also, the hypersonic solution cannot be calculated with this theory due to the introduction of nonlinear terms. However, aerodynamic coefficients computed at $M_\infty = 5.0$ can be frozen and can be used for hypersonic application. Viscous drag due to the skin friction is not computed by this program. This effect was added in a separate analysis. The resulting aerodynamic coefficients are plotted versus flight Mach number on Figure 11.

Maximum lift/drag and corresponding lift coefficients and angle of attack versus Mach number are given on Figure 12.

- Subsonic: $(L/D)_{max} \simeq 16.0$ at $\alpha \simeq 1.0$, $C_L \simeq 0.22$
- Supersonic: $(L/D)_{max}$ from 5.4 to 4.0 at $4.5° \leq \alpha \leq 6.2°$
- Hypersonic: For airbreather-OFF, rocket only $(L/D)_{max} \simeq 3.4$

More detailed aerodynamic characteristics are reported in Document 1.

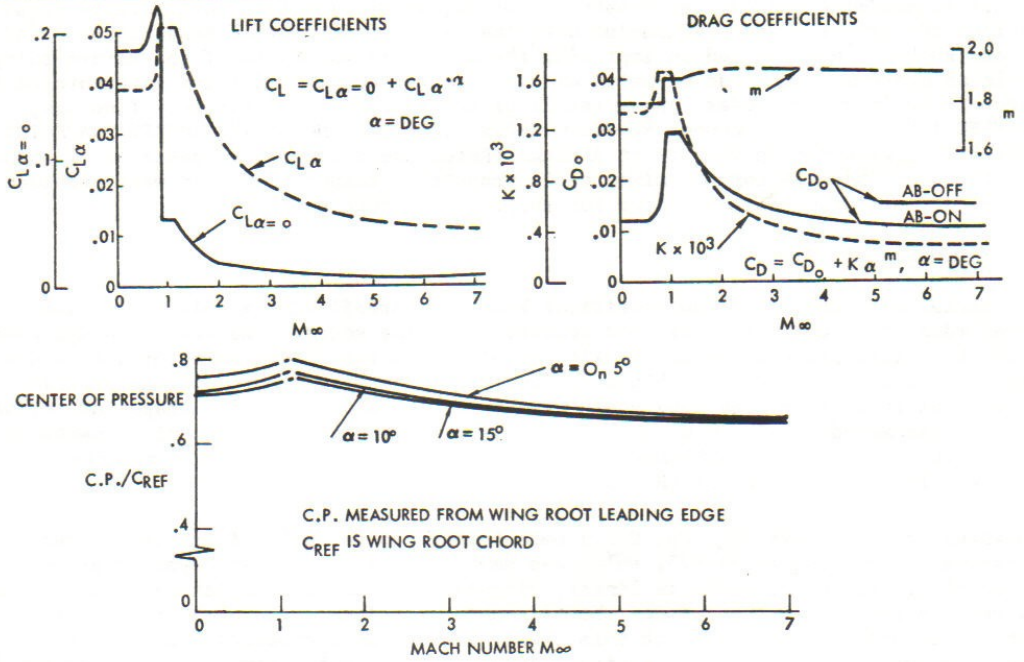

Figure 11. Aerodynamic Coefficients

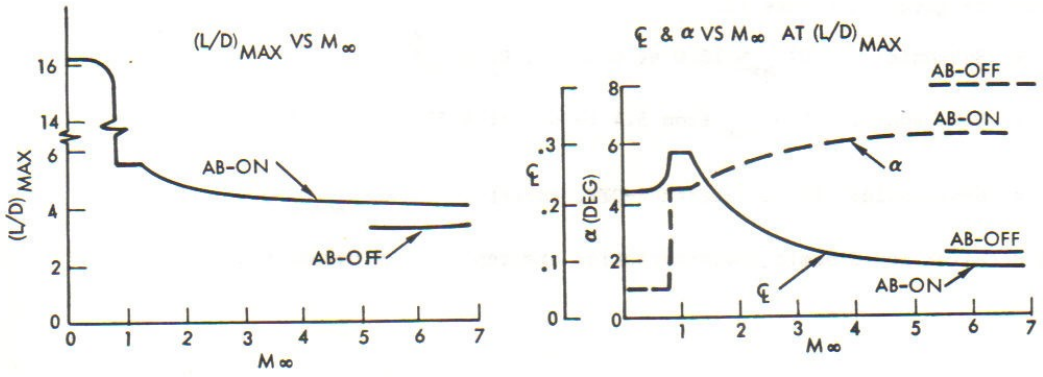

Figure 12. Maximum Lift/Drag

The wing bending moments are based on the following data:

- Differential pressure distributions computed by the Unified Distributed Panel Program
- X = 10°
- 2 g loading on wing
- GLOW = 4×10^6 lb

Lift force (L_F) and bending moment (BM) at the wing root for the above conditions are tabulated below.

M_∞	$L_F \times 10^{-6}$ lb	BM $\times 10^{-6}$ ft-lb
0.5	4.0	318
0.8	4.0	322
1.2	3.94	334
2.0	3.87	278
3.0	3.8	251
5.0	3.0	185

FLIGHT MECHANICS

The majority of the ascent performance analysis for the Star-Raker vehicle concept was accomplished using a recently developed lifting ascent program based on a modified Rutowski Energy Method (Idawa Method). This technique accurately estimated payload and propellant performance; however, it did not provide a bona fide integrated time history of trajectory state from liftoff to orbit insertion. A second computer program, the Two-Dimensional Trajectory Program (TDTP), was then used to compute the ascent trajectory timeline.

In order to do an end-to-end simulation of the Star-Raker (i.e., airbreather horizontal takeoff, climb, cruise, turn, airbreather ascent, rocket ascent, coast, and final orbit insertion) with flight optimization including aerodynamic effects, Rockwell acquired the Langley POST computer program (program to optimize simulated trajectories, developed by Martin-Marietta). POST was installed on the CDC system at Rockwell and several launch cases were executed.

The Star-Raker uses aircraft-type flight from airport takeoff to approximately Mach 6, with a parallel burn transition of airbreather and rocket engines from Mach 6 to 7.2,

and rocket-only burn from Mach 7.2 to orbit. Figure 13 illustrates a nominal trajectory from KSC to 300-nmi earth equatorial orbit. Prime elements of the trajectory are:

- Runway takeoff under high-pass turbofan/airturbo exchanger (ATE)/ramjet power, with the ramjets acting as supercharged afterburners
- Jettison and parachute recovery of landing gear used only for launch
- Climb to optimum cruise altitude with turbofan power
- Cruise at optimum altitude, Mach number, and direction vector to earth's equatorial plane, using turbofan power
- Execute a large-radius turn into the equatorial plane with turbofan power
- Climb subsonically at optimum climb angle and velocity to an optimum altitude, using high bypass turbofan/ATE/ramjet (supercharged afterburner) power
- Perform an optimum pitch-over into a nearly constant-energy (shallow γ-angle) dive if necessary, and accelerate through the transonic region to approximately Mach 1.2, using turbofan/ATE/ramjet (supercharged afterburner) power
- Execute a long-radius optimum pitch-up to an optimum supersonic climb flight path, using turbofan/ATE/ramjet power
- Climb to approximately 29 km (95 kft) altitude, and 1900 m/s (6200 fps) velocity, at optimum flight path angle and velocity, using proportional fuel-flow throttling from turbofan/ATE/ramjet, or full ramjet, as required to maximize total energy acquired per unit mass of fuel consumed as function of velocity and altitude

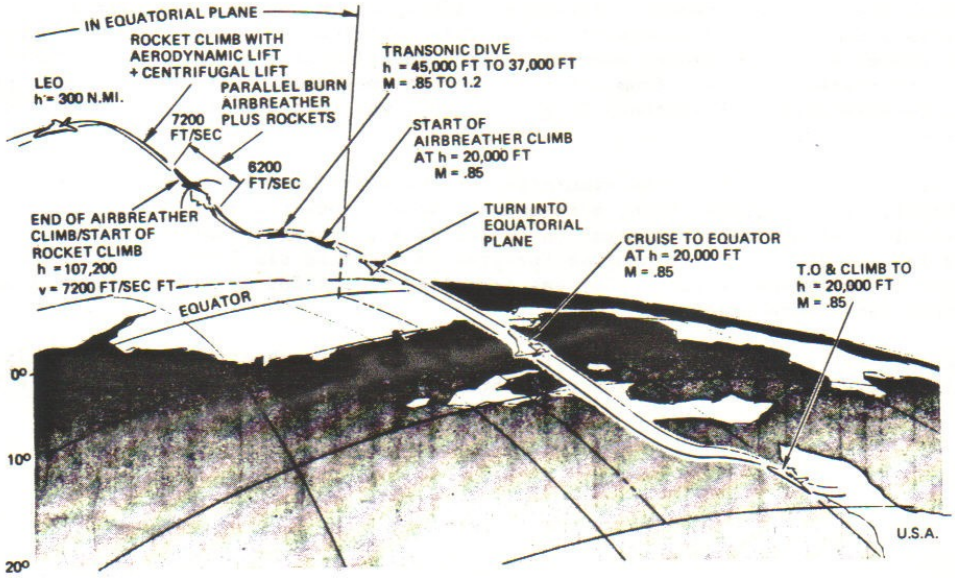

Figure 13. Star-Raker Trajectory

- Ignite rocket engines to full required thrust level at 6200 fps and parallel burn to 7200 fps
- Shut down airbreather engines while closing airbreather inlet ramps
- Continue rocket power at full thrust
- Insert into an equatorial elliptical orbit 91 x 556 km (50 x 300 nmi) along an optimum lift/drag/thrust flight profile
- Shut down rocket engines and execute a Hohmann transfer to 556 km (300 nmi)
- Circularize Hohmann transfer

The re-entry trajectory is characterized by low gamma (flight path angle) high alpha (angle of attack) similar to Shuttle. The main re-entry trajectory elements are:

- Perform delta velocity (ΔV) maneuver and insert into an equatorial elliptical orbit 91 x 556 km (50 x 300 nmi)
- Perform a low-gamma, high-alpha deceleration to approximately Mach 6.0
- Reduce alpha to maximum lift/drag (L/D) for high-velocity glide and cross-range maneuvers to subsonic velocity (approximately Mach 0.85)
- Open inlets and start some airbreather engines
- Perform powered flight to landing field, land on runway, and taxi to dock

Flyback fuel requirements include approximately 300 nmi subsonic cruise and two landing approach maneuvers (first approach waveoff with flyaround for second approach).

Typical I_{sp} characteristics of AB/rocket engine system are:

- Subsonic range - Linear reduction of I_{sp} from 9700 to 4000 sec at 1200 fps
- Supersonic range - Reduction of I_{sp} from 4000 sec at 1200 fps to 3500 sec at $\approx$ 5600 fps (AB)
- Rocket - I_{sp} = 455 sec

Required takeoff distances for the Star-Raker were compared with existing data. The distance computed for a tire rolling coefficient $\mu = 0.10$ agrees with the existing data. Throw weight sensitivity to tire rolling coefficient is 700 lb (reduction) from $\mu = 0.02$ to 0.20.

The airbreather cruise mode, which results in an economical orbit plane change from the launch site to the equatorial orbit, was analyzed. The estimated fuel requirements to cruise 1000 statute miles down-range for alternate propulsion modes are given below.

V (ft/sec)	Altitude (k-ft)	Δt (sec)	ΔW_F (lb)	Engine
800	20	6600	72,000	Turbofan Jet
6000	85	880	386,000	Ramjet

Although subsonic cruise takes a longer time (110 minutes), the amount of fuel consumed is substantially less when the orbital plane change is accomplished with subsonic cruise at maximum L/D.

A transition maneuver from high-lift configuration to $(L/D)_{max}$ configuration is performed shortly after liftoff (beginning at 3000 ft altitude). The maximum angle of attack of 13 degrees is reduced gradually to 1 degree for subsonic $(L/D)_{max}$ climb configuration.

Velocity and angle of attack vs flight time are reported in Document 1. The time required to reach 300 nmi orbit (not including subsonic cruise leg) varies from 1800 to 2300 sec, depending upon $(W/S)_0$, (T/W), and engine operational mode.

Variation in load factor, altitude, and dynamic pressure with respect to velocity and time during supersonic ascent are also reported in Document 1. The load acceleration remains less than 2.3 g (76% of Shuttle maximum acceleration), which is a comfortable level for both crew and payload. Maximum dynamic pressure is 940 psf, which is within load limits. From takeoff to burnout, the ascent profile is quite shallow - with flight path angle ranging between -0.7 and 4.5 degrees.

Ascent and descent trajectories of the Star-Raker and the Space Shuttle missions are compared in Figure 14. Because the performance of airbreathing engines and aerodynamic lifting of winged vehicle depend on the high dynamic pressure, the Star-Raker flies at much lower altitude during the powered climb than the vertical ascent trajectory of the Space Shuttle for a given flight velocity. Light wing loading of the Star-Raker contributes to the rapid deceleration during deorbit.

The total enthalpy flux histories which indicate the severity of expected aerodynamic heating are shown in Figure 14. As expected, the aerodynamic heating of ascent trajectory may design the Star-Raker TPS requirement. The maximum total enthalpy flux of 6000 Btu/ft^2-sec is estimated near the end of airbreather power climb trajectory. Except in the vicinity of vehicle nose, wing leading edge, or structural protuberances, where interference heating may exist, most of the ascent heating is from the frictional flow heating on the relatively smooth flat surface.

The descent heating is mainly produced by the compressive flow on the vehicle windward surface during the high-angle-of-attack re-entry, and is expected to be considerably lower than the Space Shuttle re-entry heating.

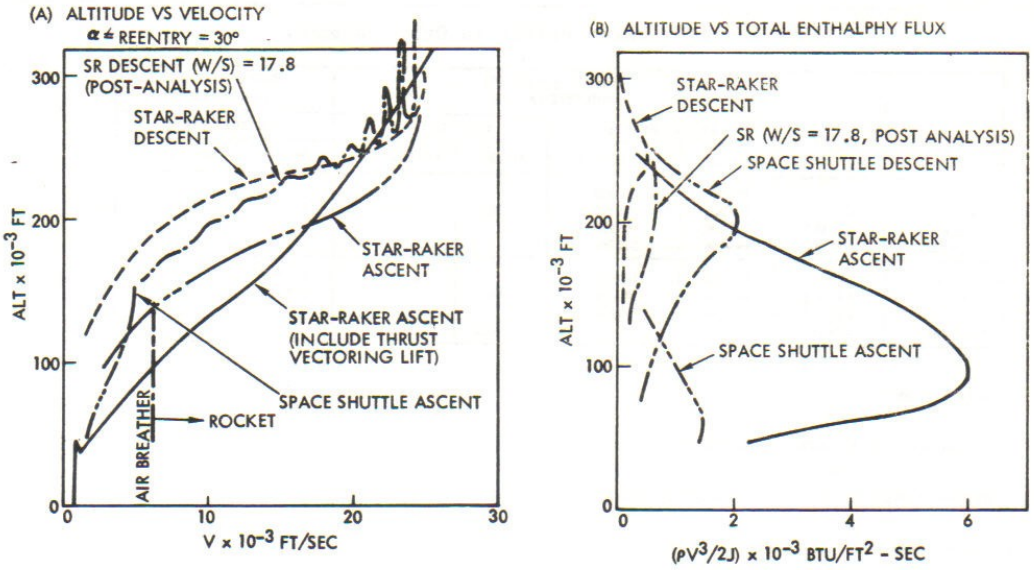

Figure 14. Ascent and Descent Trajectory Comparisons

Weight in orbit is summarized in Table 1. The data entries identified by an asterisk are revised reference vehicle data resulting from Rockwell and NASA/MSFC data exchange in May 1978. Calculations reflect additional fuel reserves, performance losses and a 10-percent growth factor. Inert weight in orbit was increased from 694,510 lb to 775,800 lb and airbreather engine thrust of 1.4×10^6 lb constant was revised to reflect increase in airbreather thrust potential shown on Figure 9.

AERODYNAMIC AND STRUCTURAL HEATING

Preliminary aerodynamic heating evaluation of the Star-Raker configuration was performed for several wing spanwise stations and the fuselage centerline.

For the wing lower surfaces, heating rates were computed including the chordwise variation of local flow properties. Effects of leading edge shock and angle of attack were included in the local flow property evaluation. Leading edge stagnation heating rates were based on the flow conditions normal to the leading edge neglecting cross-flow effects. All computations were performed using ideal gas thermodynamic properties.

Wing upper-surface heating rates were computed using free-stream flow properties, i.e., neglecting chordwise variations of flow properties. Heating rates were computed for several prescribed wall temperatures as well as the reradiation equilibrium wall temperature condition. Transition from laminar to turbulent flow was taken into account in the computations. Wing/body and inlet interference heating effects were not included in this preliminary analysis. The analysis was limited to the ascent trajectory, since the descent trajectory is thermodynamically less severe.

Table 1. Star-Raker Weight in Orbit Summary

ORBIT	GLOW $W_0 \times 10^{-6}$ LB	ROCKET I_{SP} = 455. SEC (SHUTTLE VALUES)				ROCKET I_{SP} = 468 SEC (LaRC VALUES)	
		ENERGY METHOD		POST ANALYSIS		ENERGY METHOD	
		W_f (LB)	PAYLOAD (LB)	W_f (LB)	PAYLOAD (LB)	W_f (LB)	PAYLOAD (LB)
EQUATORIAL ORBIT CRUISE FROM KSC	4.31 4.31 (P.B) 4.62 (P.B) 5.00 (P.B)	787,400. 801,700. 845,800. 895,300.	92,890. 107,190. 151,290. 200,790.	790,000.	95,490.	832,800.	138.290.
INCLINED ORBIT KSC DUE EAST	4.31 4.31 (P.B) 4.62 (P.B) *5.00 (PB)	864,500. 882,600 925,100.	169,990. 188,090. 230,590.	849,000. *972,400	154,490 *196,580	897,000. 917,300.	202,490. 222,790.

- DATA FOR 300 N.MI. ORBITAL INSERTION
- REFERENCE WING AREA (S_{REF}) = 40,900. SQ. FT.
- WEIGHT IN ORBIT (EXCLUDING PAYLOAD) = 694,510. LB * = 775,800 LB
- LAUNCH FROM KSC
- PB = PARALLEL BURN
- AIRBREATHER
  - THRUST = 1.4×10^6 LB.
  - I_{SP} = VARIABLE
  - VELOCITY = $0 \leq V \leq 6200$ FT/SEC
- ROCKET
  - THRUST = 3.2×10^6 LB
  - I_{SP} = SEE CHART
  - VELOCITY = $6200 \leq V \leq V_{ORBIT}$ FT/SEC

These parametrically generated aerodynamic heating rate data were used for thermal analysis of the various candidate insulation systems. Radiation equilibrium temperatures for emissivity, $\varepsilon = 0.85$, are based on:

- Leading edge stagnation heating rates peak at M = 16.4, alt = 196,000 ft
- Upper wing surface uniform static pressure assumed, temperatures peak at M = 6.4, alt = 86,500 ft
- Lower wing surface heating rates and temperatures peak at M = 7.9, alt = 116,000 ft
- Local flow property variation, angle of attack, and leading-edge shock effects are included
- Inlet interference effects were not included

Isotherms of the peak surface temperatures for upper and lower surfaces (excluding engine inlet interference effects) for the Star-Raker and Orbiter are shown on Figure 15. Leading edge and upper wing surface temperatures have similar profiles. Star-Raker lower-surface temperatures are from 400°F to 600°F lower than the orbiter due to lower re-entry wing loading (23 versus 67 psf).

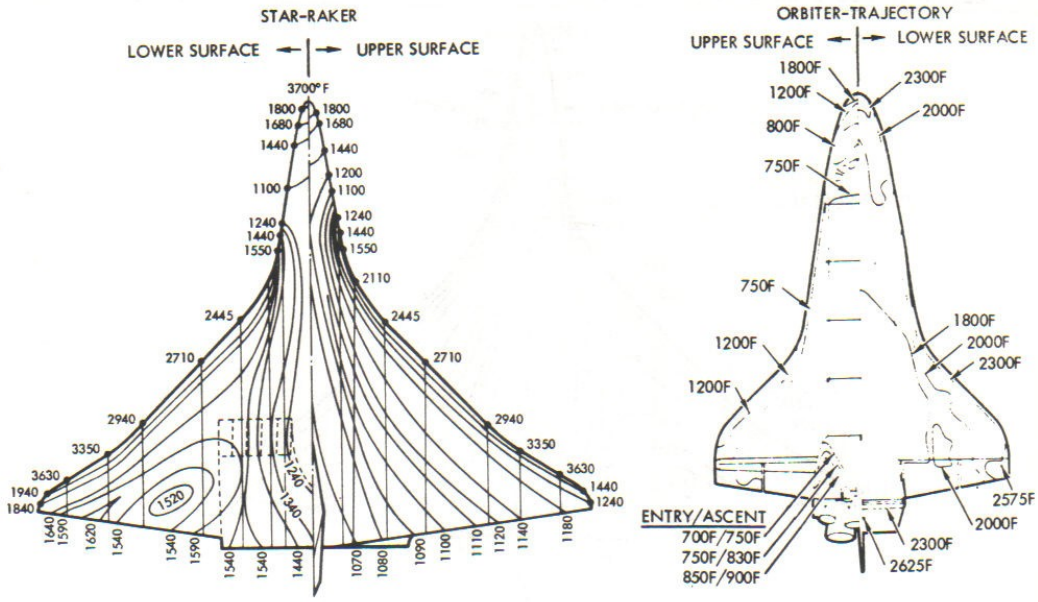

Figure 15. Isotherms of Peak Surface Temperatures During Ascent

Structural heating analysis reported in Document 1 include: (a) typical variations of heat leak rate (BTU/ft^2-hr) and total heat flux (BTU/ft^2) as a function of HRSI tile thickness for typical LH_2 upper and lower wing tank surface locations; (b) variation of bondline temperatures versus tile maximum temperature to thickness ratio for RSI tile insulation, including bondline temperatures for the dry, wingtip ullage tank, the wetted lower surface of the LH_2 tank, and the dry upper surface of the LH_2 tank; and (c) typical thermal response as a function of launch trajectory exposure time of the insulation system.

Figure 16 shows HRSI tile thickness profiles for bondline temperatures of 350F. Preliminary data indicate that the titanium aluminide system described in the TPS section of this report may be lighter than the RSI tile for the Star-Raker TPS system due to the low average temperature (1000°F to 1600°F) profiles occurring over 80 and 85 percent of the vehicle exterior surface.

THERMAL PROTECTION SYSTEM

Ceramic coated RSI tile, used on Shuttle, and metallic truss core sandwich structure, developed for the B-1 bomber, were investigated as potential thermal protection systems for Star-Raker (see Figure 6).

The radiative surface panel consists of a truss core sandwich structure fabricated by superplastic/diffusion bonding process. For temperatures up to 1500/1600°F, the concept utilizes an alloy based on the titanium-aluminum systems which show promise for high-temperature applications currently being developed by the Air Force. For temperatures higher than 1500/1600°F, it is anticipated that an alloy will be available from

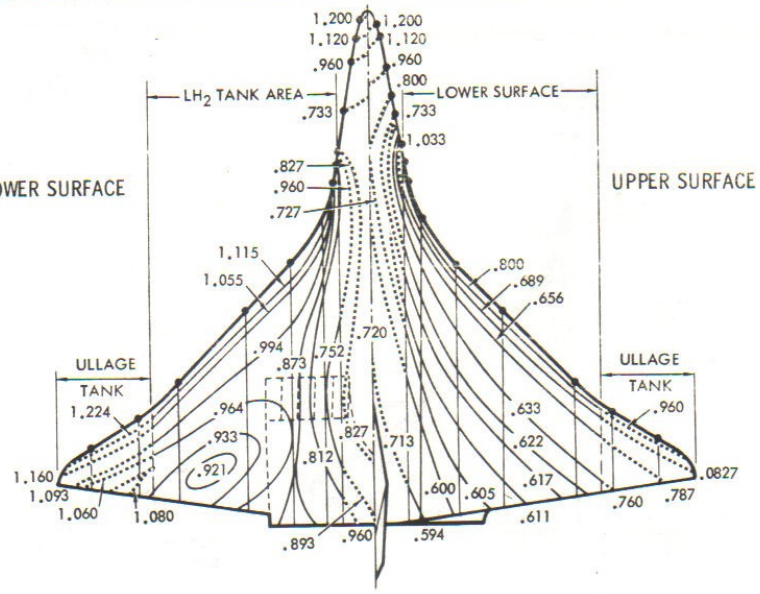

Figure 16. HRSI Tile Thickness Contours for 350°F Bonline Temperature

the dispersion-strengthened superalloys currently being developed for use in gas turbine engines. Flexible supports are designed to accommodate longitudinal thermal expansion while retaining sufficient stiffness to transmit surface pressure loads to the primary structure. Also prominent in metallic TPS designs are expansion joints which must absorb longitudinal thermal growth of the radiative surface, and simultaneously prevent the ingress of hot boundary layer gases to the panel interior. The insulation consists of flexible thermal blankets, often encapsulated in foil material to prevent moisture absorption. The insulation protects the primary load-carrying structure from the high external temperature.

During the past two years, Rockwell and Pratt and Whitney Aircraft have participated in an Air Force Materials Laboratory sponsored program, F33615-75-C-1167, directed toward the exploitation of Ti_3Al base alloy systems. The titanium aluminide intermetallic compounds based on the compositions Ti_3Al (α_2) and TiAl (λ) which form the binary Ti-Al alloys have been shown to have attractive elevated-temperature strength and high modulus/density ratios.

The titanium hardware depicted on Figure 17 is an example of complex configurations that have been developed, utilizing a process which combines superplastic forming and diffusion bonding (SPF/DB). This Rockwell proprietary process has profound implications for titanium fabrication technology, per se. In addition, the unprecedented low-cost hardware it generates promises to revolutionize the design of airframe structure. The

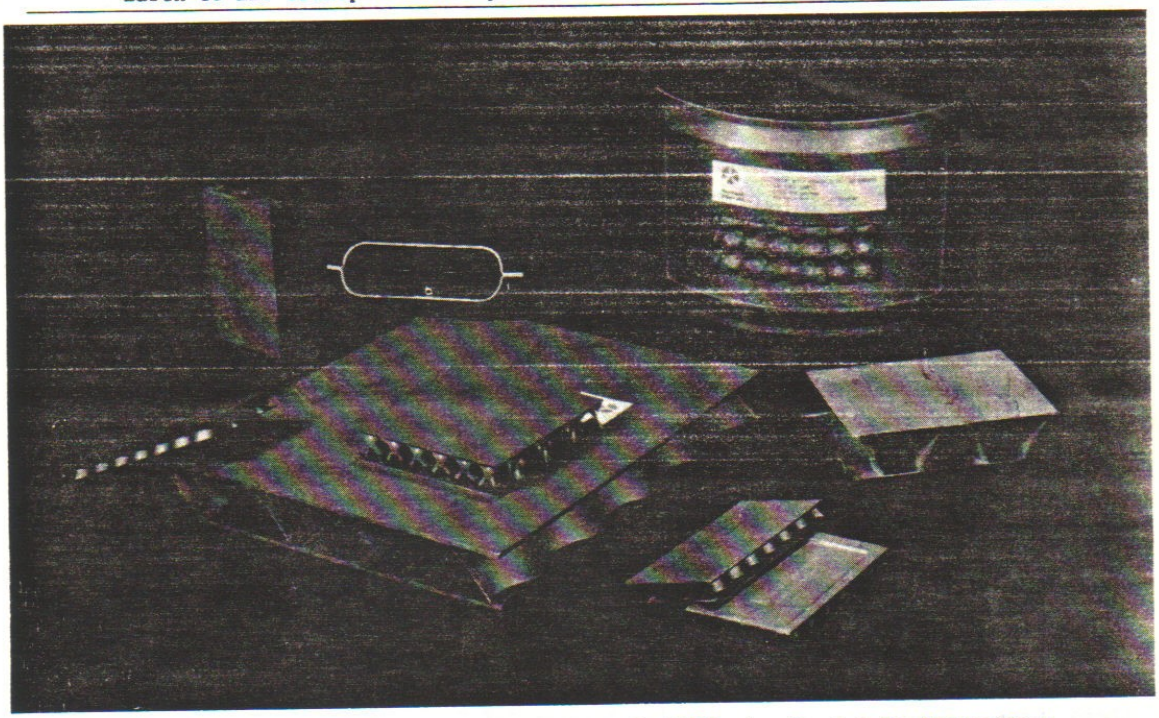

Figure 17. Examples of Super Plastic-Formed, Diffusion-Bonded Configurations

versatile nature of the process is apparent, showing complex deep-drawn structure and sandwich structure with various core configurations. This manufacturing method and the design freedom it affords offer a solution to the high cost of aircraft structure. Manufacturing feasibility and cost and weight savings potential of these processes have been established through both IR&D efforts at Rockwell and Air Force contracts. These structures may be used for engine cowling, landing gear doors, etc., in addition to providing major TPS components.

Unit masses of Star-Raker TPS concept, state-of-the-art TPS hardware and advanced thermal-structural designs are compared with the unit mass of the orbiter RSI on Figure 18. The unit mass of the RSI includes the tiles, the strain isolator pad, and bonding material. The hashed region shown for the RSI mass is indicative of insulation thickness variations necessary to maintain mold line over the bottom surface of the orbiter. The RSI is required to prevent the primary structure temperature from exceeding 350°F. The unit masses of the metallic TPS are plotted at their corresponding maximum use temperatures. The advanced designs are seen to be competitive with the directly bonded RSI.

STRUCTURAL ANALYSIS

The multi-cell wing tanks provide a structure which is capable of sustaining pressure while, at the same time, reacting aerodynamic loads. The tanks are sized based on

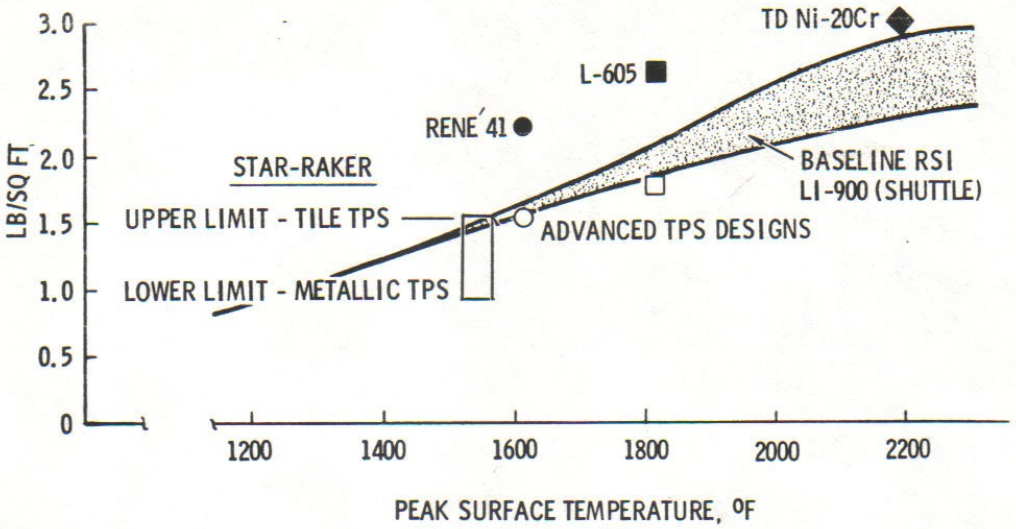

Figure 18. Unit Mass of TPS Designs

ullage pressures of 32-34 psia (LH_2) and 20-22 psia (LOX). Maximum wing bending occurs at about Mach 1.2. The LH_2 and LOX wing tanks are the major load path for reacting these loads. The wing also supports the airbreather engine system.

The primary wing attachment is to the cargo bay structure. The cargo bay aft section, in turn, is connected to the LH_2 tank. The LH_2 interconnects the cargo bay, aft portions of the wing, the vertical surface, and the rocket engine thrust structure.

An ultimate factor of safety of 1.50 was used in the analysis. The prime driver in the structural sizing of the multi-cell wing tanks is the bending moment resulting from air loads at Mach 1.2. The net bending moment on the wing is the difference between the lift moment and the relieving moment due to LOX remaining in the wing. Trades were performed to determine the structural wing weights required to sustain these bending moments plus internal pressure. An intermediate location was chosen for LOX propellant where lift moment ~2 times relieving moment. Locating LOX outboard results in a lower net flight bending moment, but the critical design condition then becomes prelaunch under full propellant loading. To sustain this prelaunch bending moment, the wing weight would be in excess of 200,000 lb.

The wing LH_2 tank was designed to sustain the loads from both internal pressure and wing bending. Al 2219-T87 was chosen for the tank material on the basis of high strength at cryogenic temperatures, fracture toughness, and weldability. Loads resulting from wing bending moments are dominant in determining membrane thickness, which is based on a maximum tank ullage pressure of 34 psia, and an ultimate factor of safety of 1.50. Figure 19 shows material thickness versus wing station due to pressure and wing bending. The column showing bending only relates to wing-bending contribution, not an unpressurized wing design.

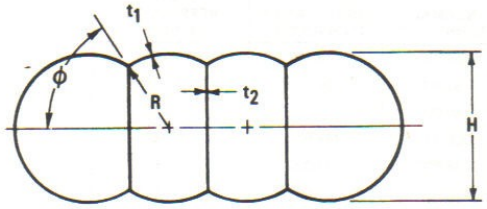

STA* (FT)	H_{NOM} (IN.)	PRESSURE REQUIREMENT $t_1 = t_2$** (IN.)	BENDING ONLY t_1 (IN.)	BENDING + PRESSURE t_1 (IN.)
10.9	240	0.066	0.021	0.087
23.0	146	0.040	0.076	0.116
54.0	110	0.031	0.092	0.123
107.0	48	0.014	0.120	0.134

*DISTANCE FROM VEHICLE ℄
**FOR ϕ = 60 DEG ONLY

Figure 19. Material Thickness Versus Wing Station

The fuselage LH_2 tank is the primary load path for reacting total vehicle mass inertias during the maximum acceleration condition (3.0 g). Approximately 27 percent of the propellant remains at that time. The tank has a twin-cone "Siamese" configuration which is required in order to fit in the fuselage at maximum propellant volume. The forward end of the tank is cylindrical, while the aft end is closed out with a double modified ellipsoidal shell. The bulkheads react the internal pressures while the sidewall carries pressure and axial compression loads. The bulkheads are monocoque construction while the sidewall is an integral skin-stringer with ring frames construction. Tank configuration and bulkhead membrane and sidewall "smeared" thickness requirements to sustain the internal pressure and axial compression loads are reported in Document 1. The structural design of all cryo tanks is based on cryogenic temperature material properties and allowables.

MASS PROPERTIES

Star-Raker mass properties are dominated by the tri-delta wing structure, the thermal protection system and the airbreather and rocket propulsion system. The initial Reference Vehicle data, shown in Table 2, were generated by Rockwell during the period of December 1977 – January 1978. These data were reviewed by NASA MSFC/LaRC during February and March 1978, resulting in two extremes of mass estimates. Cooperative effort between Rockwell and NASA teams during May produced the final reference vehicle data. The data presented in this report are considered to be reasonable achievable targets. Both Rockwell and NASA team members agree that technology items coded on Figure 1 require study in greater depth and degree of sophistication to confirm Star-Raker mass property data. Vehicle center-of-gravity data are detailed in Document 1. Mass centroids of individual elements, except the wing structure and TPS system, are in close agreement. Sensitivities in orbital insertion weight due to rocket thrust, aerodynamic lift/drag ratio, and airbreather engine thrust/weight ratio also appear in Document 1.

ORBIT DETERMINATION

Star-Raker vehicles will be rendezvousing with facilities in low earth orbit at a high rate in support of SPS. One important consideration during orbit determination is the

Table 2. Star Raker Weight Summary

ITEM DESCRIPTION	ROCKWELL	MSFC		ROCKWELL/MSFC
	INITIAL REFERENCE VEHICLE	NORMAL TECHNOLOGY	ACCELERATION TECHNOLOGY	FINAL REFERENCE VEHICLE
AIRFRAME, AEROSURFACES, TANKS AND TPS	367,000	458,000	249,000	370,000
LANDING GEAR	27,700	53,000	39,000	27,700
ROCKET PROPULSION	63,700	40,000	40,000	71,700
AIRBREATHER PROPULSION	148,000	200,000	148,000	140,000
RCS PROPULSION	4,000	16,000	11,000	10,000
OMS PROPULSION	1,200	9,000	7,000	5,000
OTHER SYSTEMS	35,500	41,000	22,000	37,800
SUBTOTAL	647,100	817,000	516,000	662,200
10% GROWTH		81,700	51,600	66,220
TOTAL INERT WEIGHT (DRY WEIGHT)	647,100	898,700	567,600	728,420
USEFUL LOAD (FLUIDS, RESERVES, ETC.)	47,400	—	—	47,400
INERT WEIGHT & USEFUL LOAD	694,500	—	—	775,820
PAYLOAD WEIGHT	107,200			196,580
ORBITAL INSERTION WEIGHT	801,700	—	—	972,400
PROPELLANT ASCENT	3,438,080			4,027,600
GLOW (POST-JETTISON LAUNCH GEAR)	4,239,780	—	—	5,000,000

300 NMI EQUATORIAL ORBIT
NOTE: THIS VEHICLE HAS 51,000 CU FT EXCESS PROPELLANT TANK VOLUME SEE WEIGHT IN ORBIT SUMMARY

300 NMI, 28.5° INCLINED ORBIT

accuracy of the resulting ephemeris prediction with time. Ephemeris accuracy depends upon initial state errors prior to the tracking period, the number of observation sets, the errors inherent in the tracking system, errors that occur during orbital maneuvers, and model errors in the satellite environment.

During CFY 1978, existing TRACE computer program options that were of interest were exercised. For each program option, the approach was to set up the required input data instructions, debug the input data deck, and to run TRACE on the in-house IBM computer system. Preferred options are:

1. General prediction accuracy derived from a combination of ground- and space-based tracking networks.

2. Orbit insertion dispersion analysis due to transfer errors (e.g., initial state, motor impulse, and attitude errors).

3. Modeling of the tracking network for orbit determination and ephemeris prediction accuracy.

1,200,000-LB STAR-RAKER/RASV COMPARISON

Performance trades were developed and comparisons made for: (a) a scaled-down version of the Star-Raker with its airbreather/rocket (AB/R) propulsion, and (b) the Reusable Aerodynamic Space Vehicle (RASV) with its all-rocket propulsion, as defined by Boeing in Reference (6). The study responded to an expression of interest by the SAMSO, who had sponsored the RASV study. The objectives were to determine whether the AB/R

configuration could achieve specific performance goals, to identify key operational and performance differences between the AB/R and all-rocket vehicles, and to determine conditions (cross-over) at which performance gains are realized.

Vehicle configurations, major design characteristics and performance groundrules to permit comparisons of useful payload are summarized in Figure 20. The scaled-down AB/R Star-Raker has a tri-delta flying wing planform (blended fuselage-wing) and a Whitcomb airfoil section similar to the Star-Raker designed for the SPS mission. This combination offers an efficient aerodynamic shape from a performance standpoint while minimizing shifts in aerodynamic center of pressure and maximizing propellant volumetric efficiency. Holding the same gross lift-off weight (GLOW) for the comparison was a study groundrule. The higher empty weight for the scaled-down or mini Star-Raker represents the addition of airbreathing engine system and net propellant tank weight increments to the basic RASV weight. As noted, the RASV has a 10,000-pound payload capability to a 100 nmi polar orbit and a 25,000-pound capability to a 100 nmi orbit at 28 degrees. The payload capability of the mini Star-Raker was to be defined parametrically.

Optimal trajectories for HTO/SSTO concepts using combined airbreathing rocket (AB/R) and all rocket propulsion systems were determined as reported in Document 2. Approximately 1500 sec of AB operation are required for the AB/R system to reach a transitional velocity ($V_{AB/R}$) of 6000 ft/sec., while 300 seconds are required by the rocket system to reach the same velocity. After $V_{AB/R}$ the time increment required to reach orbital velocity is the same for both vehicles. The corresponding aerodynamic heating parameters, which are proportional to total enthalpy flux histories, were also determined as reported in Document 2. The data show that the AB/R system will be exposed to a higher heating

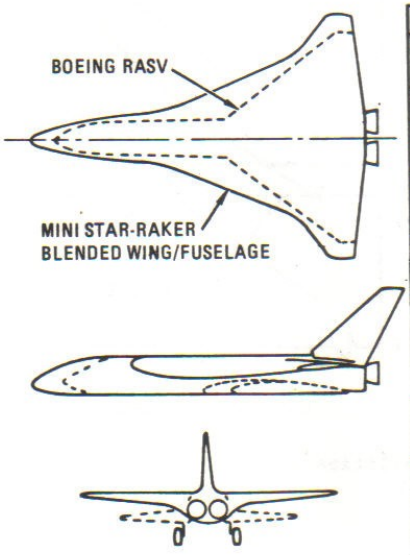

ITEM	MINI STAR-RAKER	RASV (BOEING)
GLOW:	1.2 X 10^6 LB + LAUNCHER PROP	1.22 X 10^6 LB + LAUNCHER PROP
W_E (LESS P/L):	202,000 LB (NOM)	139,000 LB
$W_{P/L}$ POLAR:	VARIABLE	10,000 LB
28 DEGREES:	VARIABLE	25,000 LB
WING S_{REF}:	8,000 FT^2	5,632 FT^2
S_{EXP}:	5,600 FT^2	4,000 FT^2
TANK VOL LOX:	9,750 FT^3	13,807 FT^3
LH_2:	62,000 FT^3	37,453 FT^3
AB ENGINES T_{MAX}:	400,000 LB	–
$I_{SP_{MAX}}$:	4,000 SEC (FOR ACCEL)	–
LIFT-OFF MODE	HORIZONTAL TAKE-OFF (HTO)	
GROUND-ASSIST TAKE-OFF VELOCITY	–	500 FPS
100 NMI CIRCULAR ORBIT (KSC POLAR AND DUE-EAST LAUNCH IN A 28° INCLINED ORBIT)		

Figure 20. Configuration Characteristics and Ground Rules

environment than the all-rocket system because the AB/R system must fly at lower altitudes where the AB engine operates most efficiently.

Total throw weight as a function of launch wing loading and AB/R transitional velocity ($V_{AB/R}$) are also presented in Document 2. For a given transitional velocity, the throw weight increases rapidly between 100 and 150 psf wing loading but flattens out between 150 and 200 psf. Therefore, considering the substantial increase in the aeroheating parameter between 150 and 200 psf, a wing loading of 150 psf was selected for the rest of the trade studies.

The useful payload capability for the AB/R system, which considers the added weight penalty resulting from AB engines and increased tank weights, is shown parametrically in Figure 21. For the AB/R configuration, the minimum payload requirement of 10,000 lb to a polar orbit can be met with a $V_{AB/R}/(T/W)_{AB}$ combination of 4000/10, 4500/8, or 6000/6. The payload requirement for 30,000 lb into the 28-degree inclined orbit is also exceeded by these engine performance/weight combinations. Figure 21 also shows that the payload capability of advanced technology AB engines of Mach 6 and $(T/W)_{AB} = 8$ are almost double those of a vehicle with state-of-the-art 40,000 lb thrust Mach 4 engines ($8 \leq (T/W)_{AB} \leq 10$). However, $(T/W)_{AB}$ will tend to decrease as $V_{AB/R}$ increases due to the added weight incurred by engine and inlet design complexities resulting from aeroheating effects.

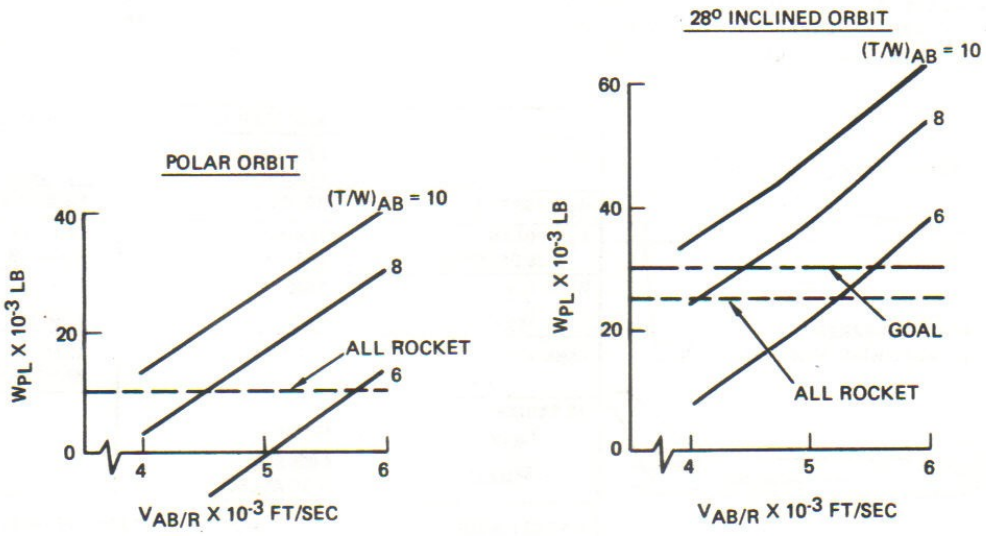

Figure 21. Payload to Orbit Capabilities of Mini Star-Raker and RASV

In summary, the performance trade studies show the following:

1. The mini Star-Raker is capable of placing the desired 10,000 and 30,000 lb of useful payload into 100 nmi polar and 28 deg orbits, respectively.

2. These payload capabilities can be achieved with various combinations of $V_{AB/R}$ ranging from 4000 to 6000 fps and $(T/W)_{AB}$ ranging from 6 to 10.

3. The optimal wing loading is approximately 150 psf when performance and aeroheating effects are taken into account.

4. The mini Star-Raker is competitive from a performance standpoint with the all-rocket RASV system with moderate advancements in AB propulsion system technology (T/W_{AB} = 8-10, and $V_{AB/R} \tilde{=}$ 4000 fps).

5. The mini Star-Raker offers the potential of major growth in payload capability (e.g., $\tilde{=}$ 25,000 lb into polar orbit and $\tilde{=}$ 50,000 lb into 28 deg orbit) with significant AB propulsion system technology advancement to $V_{AB/R}$ = 6000 fps and (T/W_{AB} < 8).

6. Key technical areas for further analysis and research are: advanced air-breathing propulsion system, TPS, wet wing, and vehicle mass fraction analysis.

A major advantage of the AB/R system is operational flexibility. Particularly, the atmospheric cruise capability with AB engines make this vehicle an excellent air transportation system for ferrying and payload pick-up missions. This capability results in reduced ground and auxiliary air transportation requirements for logistics support. The mini Star-Raker without LOX, which is required for space operation only, weighs approximately 300,000 lb (W/S $\leq$ 40 psf) including the payload and cruise fuel for 4000 statute miles. Therefore, the mini Star-Raker can operate in this mode from any airfield which can handle the C-5A or the Boeing 747 and which adds LH_2 facilities.

APPLICATION OF RESULTS

A large part of the study was performed to an accelerated schedule in order to provide results to NASA/MSFC in a briefing by the end of January 1978. NASA, in turn, provided an agency evaluation of the Star-Raker results to Rockwell personnel at the MSFC in April 1978. Major differences were resolved during the next two months. Results of the Star-Raker study were utilized in the SPS contract (NAS8-32475). Highlights were included in the SPS final report, Reference 1. Adjusted results were subsequently utilized in the SPS contract extension. As an outgrowth of the Rockwell and NASA/MSFC study and evaluation activities, NASA/MSFC let a contract, number NFT-01-002-099, subject: "Airbreathing Engine/Rocket Trajectory Optimization" to the University of Alabama.

PROJECT TITLE
Earth-to-LEO Transportation System for SPS

In March 1978, Rockwell briefed Col. Grover and Col. Graetch and staff on Star-Raker study findings. The SAMSO personnel, with support from Aerospace presented RASV data to Rockwell in March, and expressed an interest in a potential comparison of a scaled-down, 1,200,000-pound version of the Star-Raker with the RASV. Presentation of the results of the subsequent analysis, Document 2, to SAMSO is pending.

DOCUMENTATION

1. D. A. Reed, Jr., "Star-Raker, an Airbreather/Rocket-Powered, Horizontal Takeoff, Tridelta Flying Wing, Single-Stage-to-Orbit Vehicle," Rockwell Space Systems Group, Report No. SD78-AP-0044 (November 1978)

2. H. Ikawa, "Preliminary Performance and Sizing Analysis of a HTO/SSTO Vehicle with a 10 to 30 K-Lb Payload Capability," Rockwell Space Systems Group, Report No. SD78-AP-0104 (November 1978)

REFERENCES

1. "Satellite Power Systems (SPS) Concept Definition Study, NAS8-32475 Final Report," Rockwell Space Systems Group, Report No. SD78-AP-0023-5 (April 1978)

2. "Estimated Performance of a Mach 8.0 Hydrogen Fueled Turbofan Ramjet," Pratt and Whitney Aircraft Report STFRV-230A (January 1965)

3. "Air-Turborocket Application Study," Aerojet General Corporation (December 1964)

4. "Final Report and Users Manual for the Hypersonic Airbreathing Propulsion Computer Program, NASA Contract NAS2-2985," North American Aviation Reports NA66-479 and NA66-530 (May 1966)

5. Virgil K. Smith, "Airbreathing Engine/Rocket Trajectory Optimization Study," University of Alabama (August 1978)

6. "Feasibility Study of Reusable Aerodynamic Space Vehicle," SAMSO-TR-76-223, Boeing Aerospace Company (November 1976)

RELATED CONTRACT

Number	Title	Customer
NAS8-32475	Satellite Power Systems (SPS) Concept Definition Study	NASA/MSFC

Star-Raker Historical Documents Courtesy of Reed Trust

Reed Trust
914 Fairview Street
Anaheim, CA 92801
USA

Mr. Kevin Reed MSc., CMO
SESCRC/Welsom Space Power
Sattlerweg 10
94474 Seestetten/Vilshofen,
Germany
Tel. (+49) 8548/912366
Email: ReedSESCRC@yahoo.com
California Cell Phone: (+01) (714) 213-6857